Article

Cell Reports

Stimulation of the Hippocampal POMC/MC4R Circuit Alleviates Synaptic Plasticity Impairment in an Alzheimer's Disease Model

Graphical Abstract

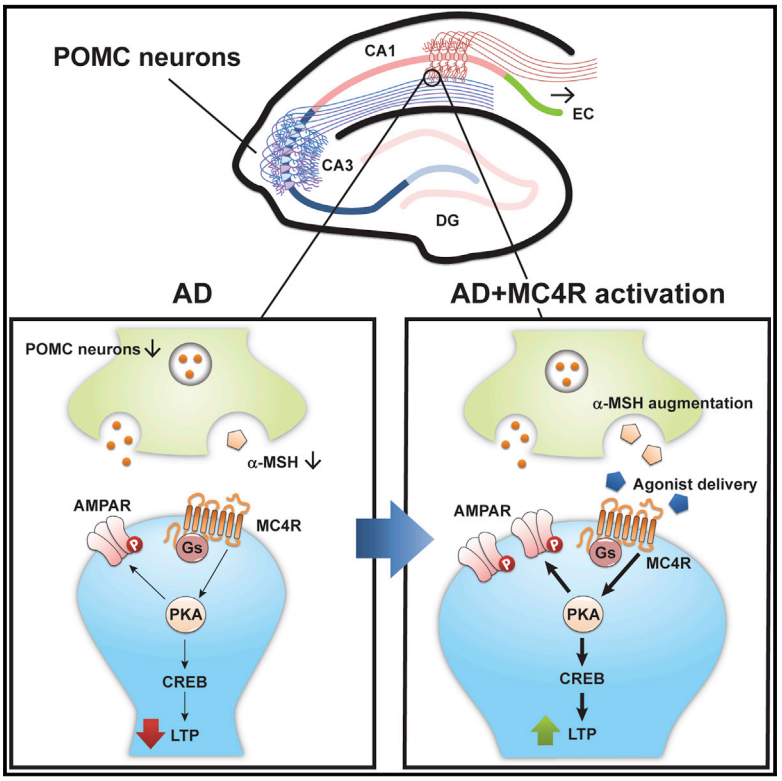

Highlights

- A functional POMC circuit in the hippocampus connects the CA3 and CA1 regions
- Lowered hippocampal MC4R activity reduces synaptic plasticity in an AD mouse model
- Activation of MC4R/Gs reverses synaptic plasticity impairment in an AD mouse model
- MC4R activation rescues Aβ-induced synaptic defects in a PKA/CREB-dependent manner

Authors

Yang Shen, Min Tian, Yuqiong Zheng, Fei Gong, Amy K.Y. Fu, Nancy Y. Ip

Correspondence

boip@ust.hk

In Brief

Shen et al. demonstrate the roles of the hippocampal POMC/MC4R circuit in synaptic plasticity impairment in an Alzheimer's disease mouse model. Suppression of hippocampal MC4R activation mediates long-term potentiation impairment in the model, whereas stimulation of the circuit restores synaptic functions.

Shen et al., 2016, Cell Reports *17*, 1819–1831
November 8, 2016
http://dx.doi.org/10.1016/j.celrep.2016.10.043

Cell Reports
Article

Stimulation of the Hippocampal POMC/MC4R Circuit Alleviates Synaptic Plasticity Impairment in an Alzheimer's Disease Model

Yang Shen,[1,2,3] Min Tian,[1,2,3] Yuqiong Zheng,[1,2,3] Fei Gong,[1,2,3] Amy K.Y. Fu,[1,2,3] and Nancy Y. Ip[1,2,3,4,*]
[1]Division of Life Science
[2]Molecular Neuroscience Center
[3]State Key Laboratory of Molecular Neuroscience
The Hong Kong University of Science and Technology, Clear Water Bay, Hong Kong, China
[4]Lead Contact
*Correspondence: boip@ust.hk
http://dx.doi.org/10.1016/j.celrep.2016.10.043

SUMMARY

Hippocampal synaptic plasticity is modulated by neuropeptides, the disruption of which might contribute to cognitive deficits observed in Alzheimer's disease (AD). Although pro-opiomelanocortin (POMC)-derived neuropeptides and melanocortin 4 receptor (MC4R) are implicated in hippocampus-dependent synaptic plasticity, how the POMC/MC4R system functions in the hippocampus and its role in synaptic dysfunction in AD are largely unknown. Here, we mapped a functional POMC circuit in the mouse hippocampus, wherein POMC neurons in the cornu ammonis 3 (CA3) activate MC4R in the CA1. Suppression of hippocampal MC4R activity in the APP/PS1 transgenic mouse model of AD exacerbates long-term potentiation impairment, which is alleviated by the replenishment of hippocampal POMC/MC4R activity or activation of hippocampal MC4R-coupled Gs signaling. Importantly, MC4R activation rescues amyloid-β-induced synaptic dysfunction via a Gs/cyclic AMP (cAMP)/PKA/cAMP-response element binding protein (CREB)-dependent mechanism. Hence, disruption of this hippocampal POMC/MC4R circuit might contribute to synaptic dysfunction observed in AD, revealing a potential therapeutic target for the disease.

INTRODUCTION

Hippocampal synaptic plasticity, manifested as long-term potentiation (LTP) and long-term depression in the hippocampal circuit, is believed to be the basis of learning and memory. LTP in the hippocampal Schaffer-collateral (SC) pathway, through which the cornu ammonis 3 (CA3) region sends information to the CA1 region for integration and processing, is the most well studied (Malenka and Bear, 2004). Synaptic plasticity in the hippocampus is modulated by different types of neuromodulators from both intrinsic and extrinsic inputs (Lemon and Manahan-Vaughan, 2006; Lin et al., 2003). Neuropeptides, one of the two major categories of neuromodulators, play a critical role in the regulation of neuronal activity. They are secreted from neural circuit inputs and specifically bind to different G-protein-coupled receptors; this modulates network activity in the long term, thus providing functional flexibility to circuits and enabling neural circuits to generate distinct output patterns (Nusbaum and Blitz, 2012). Among the various G proteins, G protein α subunit s (Gs) signaling enhances intracellular cyclic AMP (cAMP)-protein Kinase A (PKA) signaling and subsequently regulates either α-amino-3-hydroxy-5-methyl-4-isoxazolepropionic acid (AMPA)-type glutamate receptor trafficking or cAMP-response element binding protein (CREB)-dependent transcription, both of which are believed to facilitate synaptic enhancement (Banke et al., 2000). Disruption of specific neuropeptides such as neuropeptide Y disturbs hippocampal neural modulation, consequently impairing hippocampal functions as well as contributing to cognitive deficits during aging and neurodegenerative disorders such as Alzheimer's disease (AD) (Borbély et al., 2013).

The hippocampal circuit is one of the first brain regions to be affected in AD (Saxena and Caroni, 2011), and its dysfunction is believed to underlie the core features of the cognitive deficits characteristic of the disease (Palop et al., 2006). In particular, synaptic dysfunction, which disrupts vulnerable memory-related networks (La Joie et al., 2014; Selkoe, 2002), precedes neuronal degeneration and hippocampal atrophy during disease progression. Specific disruption of neuropeptides has been reported in the hippocampus in early-stage AD patients (Kapogiannis and Mattson, 2011; Saxena and Caroni, 2011). For instance, hippocampal dynorphin level is elevated in AD patients, contributing to the loss of afferents in the dentate gyrus (DG) (Ogren et al., 2010). Meanwhile, reduced somatostatin levels in the cerebral cortex and cerebrospinal fluid (CSF) have been reported in AD patients (Ogren et al., 2010). These lines of evidence suggest that neuropeptide-based modulation of neural circuitry is a possible approach for protecting the vulnerable hippocampal network and maintaining cognitive function. Although the involvement of neuropeptides

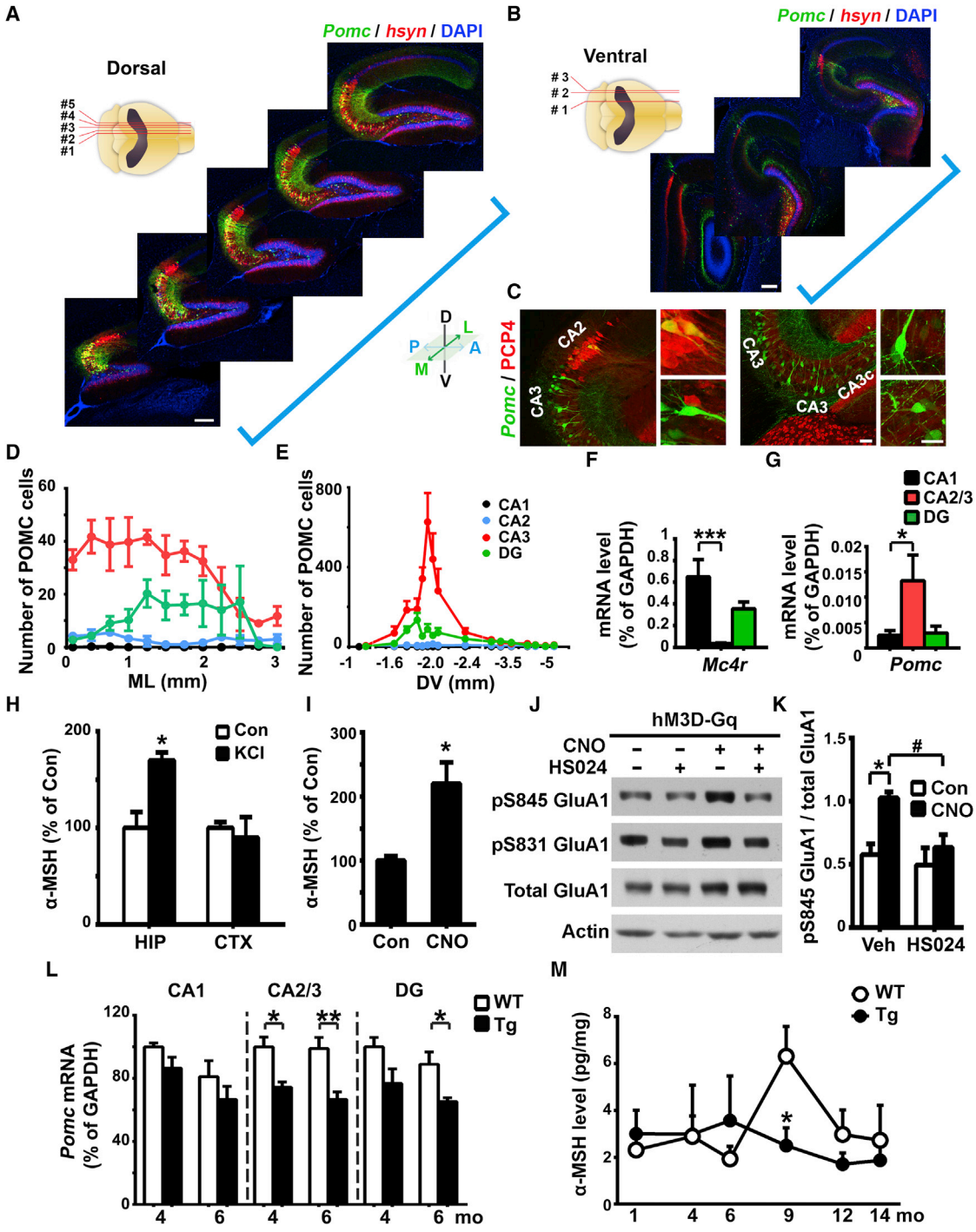

Figure 1. Functional POMC Circuit in the Mouse Hippocampus

(A–C) Labeling of pro-opiomelanocortin (POMC) neuron in *Pomc-Cre* mice by intra-hippocampal injection of Cre-dependent GFP adeno-associated virus (AAV). Cre-dependent GFP AAV and *hsyn-mCherry* AAV were co-injected to indicate the expression of virus. Serial images of GFP (*Pomc*; green), mCherry (*hsyn*; red), and DAPI (blue) in the dorsal hippocampus (A) and ventral hippocampus (B). Scale bar, 200 μm. (C) Molecular and anatomical characterization of POMC-positive cells in the CA3 region. Representative images showing co-labeling of *Pomc* (green) and PCP4. Scale bars, 100 μm (left); 50 μm (right).

(D and E) Quantitative assessment of POMC cell distribution in the mouse hippocampus. (D) Assessment along the mediolateral (ML) axis. (E) Assessment along the dorsoventral (DV) axis (mean ± SEM; n = 4–6 mice; all coordinates are relative to the bregma).

(F and G) mRNAs of different subregions of the mouse hippocampus were prepared and subjected to real-time PCR. Data are presented as the relative ratio of mRNA to that of *Gapdh*: mean ± SEM; n = 4–6 mice. (F) ***$p < 0.001$, CA1 versus CA2/3. (G) *$p < 0.05$, CA1 versus CA2/3 (one-way ANOVA with the Bonferroni post hoc test).

(legend continued on next page)

in the modulation of hippocampal synaptic plasticity during disease progression requires further detailed investigation, the development of circuit-modulating strategies is a promising strategy for early-stage AD treatment.

The neuropeptide α-melanocyte-stimulating hormone (α-MSH), which is generated from the cleavage of pro-opiomelanocortin (POMC), plays a well-established role in energy hemostasis regulation in the hypothalamus (Millington, 2007). α-MSH activates melanocortin 4 receptor (MC4R), consequently enhancing the intracellular secondary messenger cAMP via Gs activation (Barsh and Schwartz, 2002). Although MC4R is prominently expressed in the mouse hippocampus (Kishi et al., 2003), its physiological functions remain unexplored. Administration of α-MSH or its analog [Nle4,D-Phe7]-α-MSH (NDP-MSH) enhances learning and memory, and exerts a neuroprotective effect in the hippocampus (Beckwith et al., 1977; Machado et al., 2010; Sandman et al., 1980). Furthermore, activation of hippocampal MC4R by exogenous ligand administration enhances synaptic plasticity (Shen et al., 2013). These findings demonstrate the action of α-MSH/MC4R signaling in the hippocampus. Therefore, it is important to determine whether there is a hippocampal melanocortin system and, if so, how it functions. Importantly, α-MSH levels are reduced in both the plasma and the CSF of AD patients, suggesting that α-MSH-based neuromodulation is disrupted (Catania et al., 2000). Hence, it would be of interest to understand how the hippocampal melanocortin peptide system is regulated and whether the circuit is involved in the synaptic plasticity impairment in the disease.

Here, we mapped a POMC/MC4R circuit in the mouse hippocampus, the dysfunction of which causes early synaptic plasticity impairment in the amyloid precursor protein (APP)/presenilin 1 (PS1) mouse model of AD. Stimulation of CA3 POMC neurons triggers α-MSH secretion, which activates MC4R in the postsynaptic CA1 region, demonstrating the existence of a hippocampal CA3-CA1 POMC circuit. Blockade of the hippocampal α-MSH/MC4R circuit results in precocious LTP impairment in these mice, whereas activation of this circuit reverses the deficit. The positive action of the α-MSH/MC4R circuit on synaptic functions in this mouse model is mediated by the postsynaptic activation of Gs/PKA/CREB signaling. Our findings collectively demonstrate that disruption of the hippocampal α-MSH/MC4R circuit contributes to synaptic impairment in AD.

RESULTS

Functional POMC Circuit in the Mouse Hippocampus

We previously demonstrated that MC4R activation in mouse hippocampal pyramidal neurons regulates structural and functional plasticity (Shen et al., 2013). However, it is unknown how MC4R activation is regulated in the hippocampus at the circuit level, including the source of the cognate ligand of MC4R (i.e., α-MSH). As a first step to determine whether a specific hippocampal circuit is involved in MC4R activation, we examined whether POMC neurons, which generate and secrete α-MSH, are present in the mouse hippocampus. The POMC cells in the adult mouse hippocampus were labeled using *Pomc-Cre* mice, which express Cre recombinase driven by the *Pomc* promoter (McHugh et al., 2007). Recombination of injected *AAV$_9$-FLEx-GFP* in the *Pomc-Cre* mice occurred only in POMC-positive cells, indicating the localization of POMC-expressing cells (labeled with GFP) in the mouse hippocampus (Figures 1A–1C). The POMC-expressing cells were mainly observed in the CA2/3 pyramidal layers (Figures 1A, 1B, and S1A–S1F). Specifically, staining with the CA2 marker Purkinje cell protein 4 (PCP4) showed that the POMC-expressing cells were mainly localized in the CA3 region (Figure 1C). Quantitative assessment of hippocampal POMC cell distribution confirmed that the POMC cells were mainly confined to the CA3 region of the dorsal mouse hippocampus; notably, a few POMC cells were observed in the DG granule cell layer and hilus (Figures 1D, 1E, and S1G–S1J).

Real-time quantitative PCR analysis was used to confirm the presence of POMC cells in the mouse hippocampal CA3 region. Significantly higher levels of *Pomc* mRNA were detected in the CA2/3 region compared with the CA1 or DG, whereas the highest *Mc4r* transcript levels in the hippocampus were found in the CA1 (Figures 1F and 1G). Co-staining with specific neuronal markers revealed the identity of the POMC cells. Most of the POMC cells in the CA2/3 were positive for the excitatory neuronal marker calcium/calmodulin-dependent kinase II alpha subunit (CaMKIIα) but were not co-localized with several inhibitory neuronal markers (Figures S1A–S1F). Therefore, these cells are CA2/3 pyramidal cells. In contrast, the POMC cells in the hilus were positive for calretinin, but not other inhibitory markers (Figures S1G and S1H). These results together with the presence of numerous large dendritic spines at the proximal dendrites suggest that the

(H and I) Neuronal activity stimulated α-melanocyte-stimulating hormone (α-MSH) secretion from hippocampal POMC cells. (H) Adult mouse hippocampal (HIP) or cortical (CTX) slices were treated with high potassium (KCl) for 2 hr. α-MSH released by brain tissues into artificial cerebrospinal fluid (aCSF) was quantified and normalized to that of the untreated control (*$p < 0.05$, KCl versus Con in HIP, Student's t test; n = 5 experiments). (I) Firing of POMC cells in the mouse hippocampus enhanced α-MSH secretion. The specific expression of hM3Dq in hippocampal POMC-positive cells was achieved by intra-hippocampal injection of Cre-dependent hM3D-Gq AAV into *Pomc-Cre* mice. CNO administration stimulated the activation of neurons expressing hMC3Dq (*$p < 0.05$, clozapine-*N*-oxide [CNO] versus Con, Student's t test; n = 3 experiments).

(J and K) CA3 POMC cell activation enhanced GluA1 phosphorylation in an MC4R-dependent manner. (J) Hippocampal POMC cell firing enhanced pS845 GluA1 in the CA1 region. Co-treatment with HS024 abolished the increased phosphorylation (western blot analysis). (K) Quantification of band intensity (pS845 GluA1/total GluA1, *$p < 0.05$, CNO versus control [Con] in vehicle [Veh] condition, $^{\#}$CNO+HS024 versus CNO, one-way ANOVA with the Bonferroni test; n = 3 experiments).

(L and M) Vulnerability of the hippocampal POMC/MC4R circuit in APP/PS1 mice. (L) *Pomc* mRNA levels of different hippocampal subregions in APP/PS1 mice at 4 and 6 months of age. Data are presented as the relative ratio of mRNA versus *Gapdh*. *$p < 0.05$; **$p < 0.01$ versus respective wild-type (WT) group, Student's t test; n = 6 mice per group. (M) Hippocampal α-MSH levels in WT and transgenic (Tg; i.e., APP/PS1) mice upon aging (*$p < 0.05$ versus respective WT group, one-way ANOVA with the Bonferroni post hoc test; n = 4–6 mice per group).

CA1, cornu ammonis 1; CA2/3, cornu ammonis 2/3; DG, dentate gyrus.

POMC cells in the hilus are mossy cells (Scharfman and Myers, 2013) (Figures S1G–S1J). Thus, the POMC cells in the hippocampus are mainly CA3 pyramidal neurons, suggesting that they may secrete α-MSH and activate MC4R on the CA1 neurons, forming a POMC/MC4R circuit in the mouse hippocampus.

To demonstrate that this hippocampal POMC/MC4R circuit is functional, we determined whether the POMC neurons in the mouse hippocampus express and secrete α-MSH. The endogenous level of α-MSH in the mouse hippocampus was ~1.5-fold higher than that in the cortex but much lower than that in the hypothalamus (Figure S2A). Enhanced neuronal firing by high potassium treatment significantly increased α-MSH secretion in acute mouse hippocampal slices (Figure 1H). To specifically induce the selective firing of POMC neurons in the mouse hippocampus, we labeled these neurons with the stimulatory mutated muscarinic G-protein-coupled receptor (hM3D-G protein α subunit q [Gq]; DREADD-Gq [“designer receptors exclusively activated by designer drugs”-Gq]), which couples with the Gq pathway to acutely fire the neurons upon activation by the receptor ligand clozapine-*N*-oxide (CNO) (Alexander et al., 2009). The CNO-induced selective firing of the hippocampal POMC neurons significantly increased α-MSH secretion in the acute mouse hippocampal slices (Figure 1I). We subsequently examined whether stimulation of the hippocampal POMC neurons, which triggers α-MSH secretion, can activate postsynaptic MC4Rs. Accordingly, CNO treatment significantly increased the Ser845 phosphorylation of the AMPA receptor subunit GluA1, a downstream target of MC4R signaling (Shen et al., 2013) in the CA1, by ~80% (Figures 1J and 1K). Meanwhile, co-treatment with the MC4R antagonist HS024 abolished the specific increase of Ser845 GluA1 phosphorylation (Figures 1J and 1K). Stimulation of hilar POMC cells did not increase this GluA1 phosphorylation (Figures S2B and S2C). Furthermore, activation of the CA3 POMC neurons in the acute hippocampal slices from the wild-type (WT) mice increased the Ser845 phosphorylation of GluA1, whereas this increase was abolished in the heterozygous *Mc4r* null (*Mc4r*^{tm1Lowl}) mice (*Mc4r*$^{+/-}$; Figures S2D and S2E). These results collectively suggest that the stimulation of CA3 POMC neurons resulted in the secretion of α-MSH, which consequently activates MC4R and modulates the functions of its downstream effector AMPA receptor on the postsynaptic neurons, thus forming a functional “ligand-receptor system” in the mouse hippocampus.

The α-MSH/MC4R pathway plays an important role in hippocampal synaptic functions (Shen et al., 2013). Moreover, hypothalamic POMC and CSF α-MSH signaling appear to be attenuated upon aging and in AD (Catania et al., 2000; Yang et al., 2012). Therefore, we examined the regulation of the hippocampal POMC neurons upon aging in WT and APP/PS1 mice. Whereas *Pomc* mRNA levels remained relatively unchanged in different hippocampal subregions (i.e., the CA1, CA2/3, and DG) in WT mice, they were significantly reduced in the CA2/3 regions of APP/PS1 mice at 4 and 6 months of age, when synaptic dysfunction begins (Figure 1L). Soluble amyloid-beta oligomers (Aβ), which are generated by the proteolytic cleavage of APP, are believed to trigger synaptic impairment during AD progression (Larson and Lesné, 2012). Treatment with Aβ reduced the *Pomc* transcript levels in acute hippocampal slices (Figures S2F–S2H). To study the functional consequence of the loss of *Pomc* transcript in the mouse hippocampus of APP/PS1 mice, we examined the changes of α-MSH levels in the hippocampus. Accordingly, α-MSH levels increased significantly in the hippocampus of WT mice at ~9 months of age; however, this increase was abolished in APP/PS1 mice (Figure 1M).

Perturbed Hippocampal MC4R Signaling Exacerbates LTP Impairment in APP/PS1 Mice

Because α-MSH/MC4R signaling is attenuated in the hippocampus of APP/PS1 mice at the early stage of hippocampal synaptic plasticity impairment, we determined whether this decreased signaling is sufficient to trigger precocious synaptic dysfunction in younger transgenic (Tg) mice before the onset of the phenotype. There was no significant difference in the LTP at SC-CA1 synapses between APP/PS1 and control mice at 4–5 months of age (Figures 2A–2H), which indicates that there was no synaptic plasticity dysfunction in APP/PS1 mice at this age. However, ablation of POMC cells in the CA3 area by the Cre-mediated expression of diphtheria toxin receptor (DTR) followed by diphtheria toxin (DT) injection significantly reduced the magnitude of LTP at hippocampal SC-CA1 synapses, indicating that removal of the cells secreting the presynaptic ligands of MC4R in the hippocampus exacerbates the impairment of synaptic plasticity in APP/PS1 mice (Figures 2A and 2B). Moreover, chronic intracerebroventricular (ICV) infusion of selective antagonists of MC4R, including HS024 and MCL 0020, which compete with the ligand released from presynaptic neurons, also exacerbated hippocampal LTP impairment in APP/PS1 mice (Figures 2C, 2D, S3A, and S3B). To demonstrate that postsynaptic MC4R mediates the POMC/α-MSH/MC4R signaling pathway in the hippocampus, the MC4R activity in CA1 neurons was selectively blocked by overexpression of its endogenous inverse agonist, agouti-related protein (AgRP), which also significantly reduced LTP magnitude (Figures 2E, 2F, and S3C). Finally, deletion of postsynaptic MC4R in CA1 by shRNA-mediated knockdown not only reduced LTP in WT mice, but also further reduced LTP magnitude in APP/PS1 mice (by ~20% versus WT; Figures 2G, 2H, and S3D–S3G). These results collectively show that blockade of the POMC/MC4R circuit in the hippocampus accelerates and exacerbates defects in synaptic plasticity in APP/PS1 mice.

Enhanced Activation of Hippocampal MC4R Rescues LTP Impairment in APP/PS1 Mice

We subsequently investigated whether stimulation or replenishment of the POMC/MC4R circuit in the hippocampus can rescue LTP defects in these transgenic mice. Accordingly, ICV infusion of the MC4R agonist D-tyrosine (D-Tyr) melanotan-II (MTII) in APP/PS1 mice at ~6 months of age, when SC-CA1 LTP impairment is first observed, reversed such synaptic plasticity impairment (Figures 3A and 3B). Although the hippocampal LTP magnitude in APP/PS1 mice was reduced by ~16%, D-Tyr MTII administration restored the LTP magnitude to that of the WT controls (Figures 3A and 3B). Next, we determined whether the beneficial effect of D-Tyr MTII on hippocampal LTP in APP/PS1 mice is mediated by postsynaptic MC4R activation. MC4R knockdown in the CA1 region of APP/PS1 mice abolished

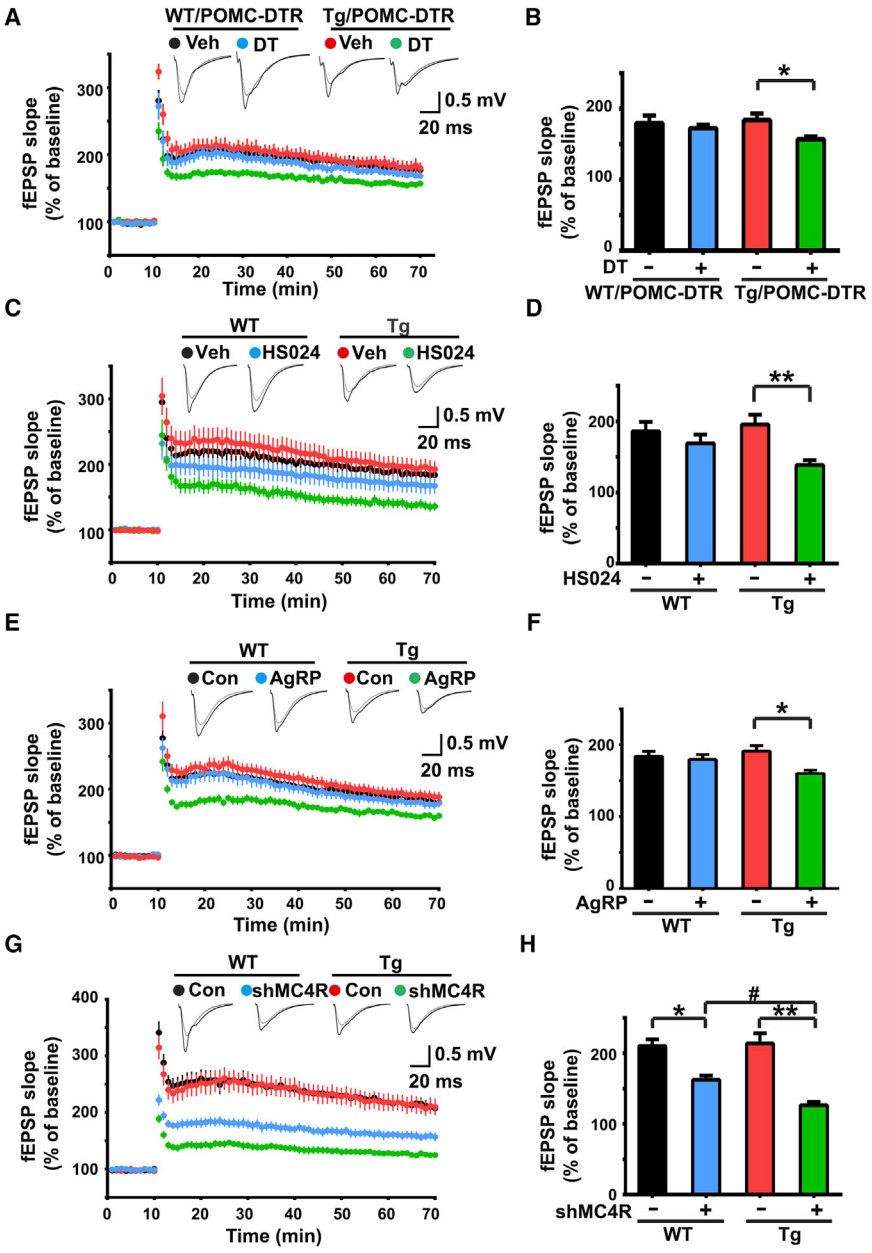

Figure 2. Perturbation of POMC/MC4R Signaling Triggers Early Deficits in Synaptic Plasticity in an AD Mouse Model

(A and B) Deletion of POMC cells in Tg (APP/PS1) mice impaired long-term potentiation (LTP) formation induced by high-frequency stimulation (HFS). Tg mice with DTR expressed in the POMC cells (Tg/POMC-DTR) and WT control mice (WT/POMC-DTR) were injected with DT to mediate the ablation of POMC cells.

(C and D) Intracerebroventricular infusion of HS024 exacerbated LTP impairment in Tg mice.

(E and F) Virus-mediated overexpression of agouti-related protein (AgRP) in the mouse hippocampus resulted in LTP impairment in Tg mice at an earlier age. The hippocampi of 3-month-old Tg mice were injected with AgRP adeno-associated virus (AAV) and kept for 7 weeks.

(G and H) Virus-mediated knockdown of MC4R in the CA1 region of Tg mice triggered the early development of LTP impairment.

(A–H) LTP in the CA1 of the Schaffer-collateral pathway was induced by two trains of HFS. (A, C, E, and G) Summary plot of normalized field excitatory postsynaptic potential (fEPSP) slope measurement. (B, D, F, and H) Quantification of mean fEPSP slopes as averaged in the last 10 min of the recording after LTP induction (mean ± SEM). (B) *$p < 0.05$, Tg/POMC-DTR DT versus Tg/POMC-DTR vehicle (Veh), one-way ANOVA with the Bonferroni post hoc test. (D) **$p < 0.01$, Tg HS024 versus Tg Veh, two-way ANOVA. (F) *$p < 0.05$, Tg AgRP versus Tg Con. (H) *$p < 0.05$, WT short hairpin RNA against *Mc4r* (shMC4R) versus WT Con; **$p < 0.01$, Tg shMC4R versus Tg Con, two-way ANOVA; $^{\#}p < 0.05$, Tg shMC4R versus WT shMC4R, one-way ANOVA with the Bonferroni post hoc test.

the D-Tyr MTII-stimulated enhancement of SC-CA1 LTP (Figures 3C and 3D). We subsequently determined whether replenishment of POMC or its cleavage product, α-MSH, in the hippocampal POMC neurons rescues the LTP impairment in APP/PS1 mice. Specific overexpression of POMC or α-MSH in the hippocampal POMC neurons of APP/PS1 mice under the control of the *Pomc* promoter (Figure S4A) restored the impaired LTP in APP/PS1 mice (Figures 3E, 3F, S4B, and S4E). MC4R knockdown in the CA1 completely abolished the POMC-mediated rescue of impaired LTP (Figures 3G and 3H). Hence, the results indicate that enhanced hippocampal POMC/MC4R signaling reverses the hippocampal synaptic plasticity impairment in APP/PS1 mice.

MC4R Activation Rescues Defects in Synaptic Morphology and Neurotransmission in the Hippocampus of APP/PS1 Mice

Dendritic spine loss and synaptic dysfunctions are directly associated with AD pathogenesis and related memory loss (Selkoe, 2002). Therefore, we investigated whether D-Tyr MTII administration can reverse the dendritic spine loss and synaptic defects in APP/PS1 mice. The percentage of mature dendritic spines and spine width in the hippocampal CA1 stratum radiatum region were significantly reduced in 6-month-old APP/PS1 mice; moreover, 4 weeks of ICV infusion of D-Tyr MTII effectively reversed these decreases (Figures 4A–4C). Furthermore, 6-month-old APP/PS1 mice exhibited significantly reduced SC-CA1 synaptic transmission strength as indicated by a decrease in the field excitatory postsynaptic potential (fEPSP) input-output (I/O) relationship. D-Tyr MTII infusion reversed the neurotransmission deficit in an MC4R-dependent manner (Figures 4D and 4E). Thus, the results indicate that MC4R activation restores dendritic spine loss

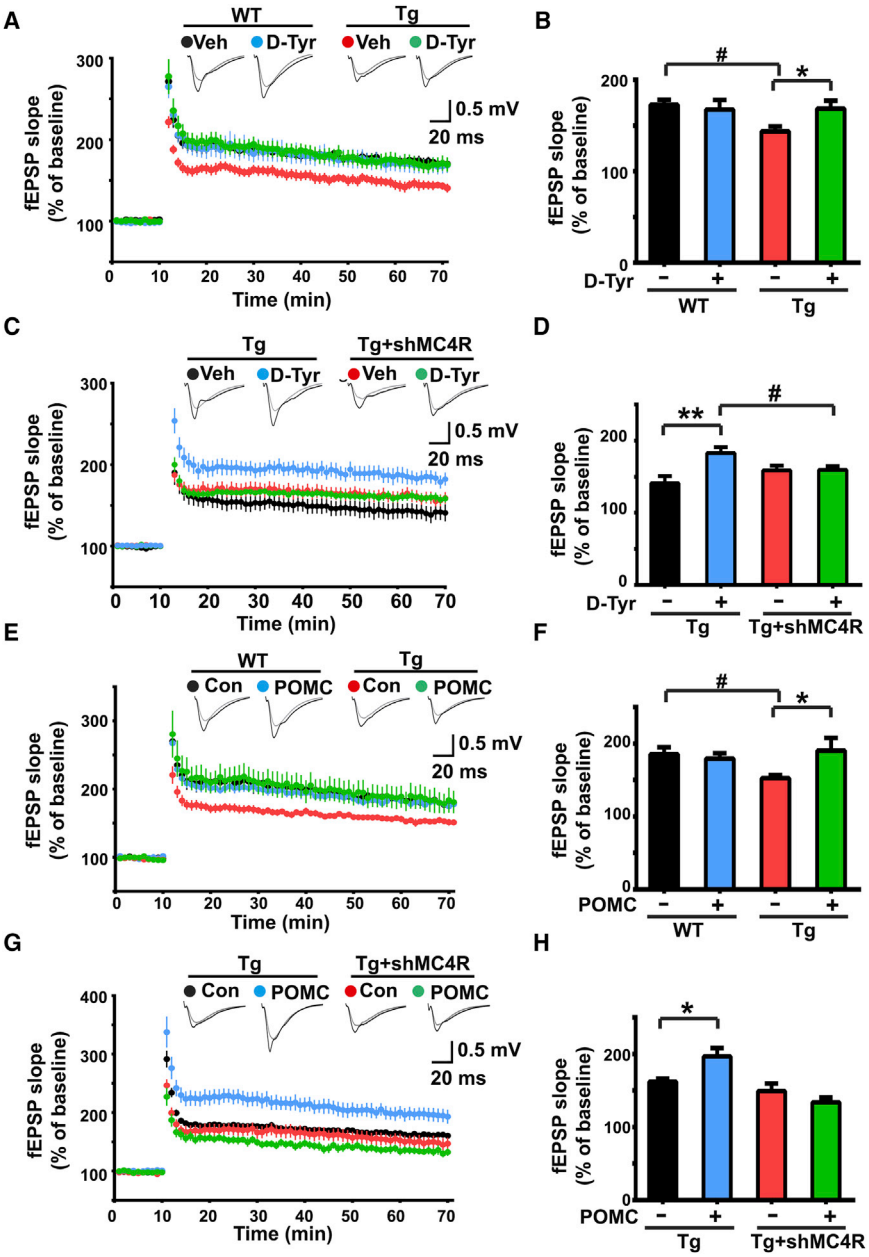

Figure 3. Activation of Hippocampal MC4R Signaling Rescues LTP Impairment in APP/PS1 Mice

(A and B) Intracerebroventricular infusion of the MC4R agonist D-Tyr (D-Tyr MTII) for 4 weeks rescued the LTP impairment in Tg mice at 6 months of age. (C and D) MC4R knockdown abolished the D-Tyr-induced rescue of hippocampal LTP impairment in Tg mice. (E–H) Overexpression of full-length POMC, specifically in hippocampal POMC cells, significantly reversed CA1 LTP impairment in Tg mice (E and F), which was abolished when MC4R was knocked down in the CA1 region (G and H). (A, C, E, and G) LTP in the CA1 of the Schaffer-collateral pathway was induced by two trains of HFS. (B, D, E, and H) Quantification of mean fEPSP slopes as averaged in the last 10 min of the recording after LTP induction (mean ± SEM). (B) $^{\#}p < 0.05$, Tg Veh versus WT Veh; $^{*}p < 0.05$, Tg D-Tyr versus Tg Veh, one-way ANOVA with the Bonferroni post hoc test. (D) $^{**}p < 0.01$, Tg D-Tyr versus Tg Veh; $^{\#}p < 0.05$, Tg + shMC4R D-Tyr versus Tg D-Tyr, two-way ANOVA. (F) $^{\#}p < 0.05$, Tg control (Con) versus WT Con; $^{*}p < 0.05$, Tg POMC versus Tg Con, one-way ANOVA with the Bonferroni post hoc test. (H) $^{*}p < 0.05$, Tg POMC versus Tg Con, one-way ANOVA with the Bonferroni post hoc test.

and basal synaptic transmission in the hippocampus of APP/PS1 mice.

Activation of MC4R-Coupled Gs Signaling Rescues LTP Impairment in APP/PS1 Mice

MC4R belongs to the G-protein-coupled receptor family, which transduces signals by coupling to the heterotrimeric Gs protein. Therefore, we determined whether activation of MC4R-coupled Gs signaling in the postsynaptic CA1 neurons is sufficient to rescue synaptic plasticity impairment in APP/PS1 mice. To selectively activate Gs signaling in the hippocampal CA1 neurons, we overexpressed rat M3-muscarinic receptor (rM3D)-Gs (DREADD-Gs) in the CA1 region (Guettier et al., 2009). Selective activation of rM3D-Gs-expressing neurons in acute mouse hippocampal slices significantly enhanced Gs signaling, as indicated by increased GluA1 phosphorylation at Ser845 (Figures S5A–S5F). In vivo activation of rM3D-Gs-expressing neurons in the hippocampal CA1 region in APP/PS1 mice by CNO injection significantly reversed the synaptic plasticity impairment in the transgenic mice at 6 months of age (Figures 5A and 5B).

Besides the activation of Gs/cAMP/PKA signaling, MC4R can enhance neuronal activity in a Gs-independent manner (Alexander et al., 2009; Ghamari-Langroudi et al., 2015). Therefore, we determined whether MC4R on postsynaptic neurons exerts its beneficial action through the modulation of neuronal activity. Direct stimulation or inhibition of the activity of CA1 postsynaptic neurons through activation of hM3D-Gq or hM4D-Di, respectively, did not rescue synaptic plasticity impairment in 6-month-old APP/PS1 mice (Figures 5C, 5D, S5G, and S5H). These results indicate that the activation of Gs signaling, but not Gq or G protein α subunit i (Gi), rescues synaptic plasticity impairment in APP/PS1 mice.

Because perturbation of hippocampal MC4R signaling exacerbated LTP impairment in APP/PS1 mice (Figure 2), we determined whether the activation of Gs signaling downstream of MC4R is sufficient to rescue this impairment. Although blockade of MC4R in the hippocampus by AgRP overexpression

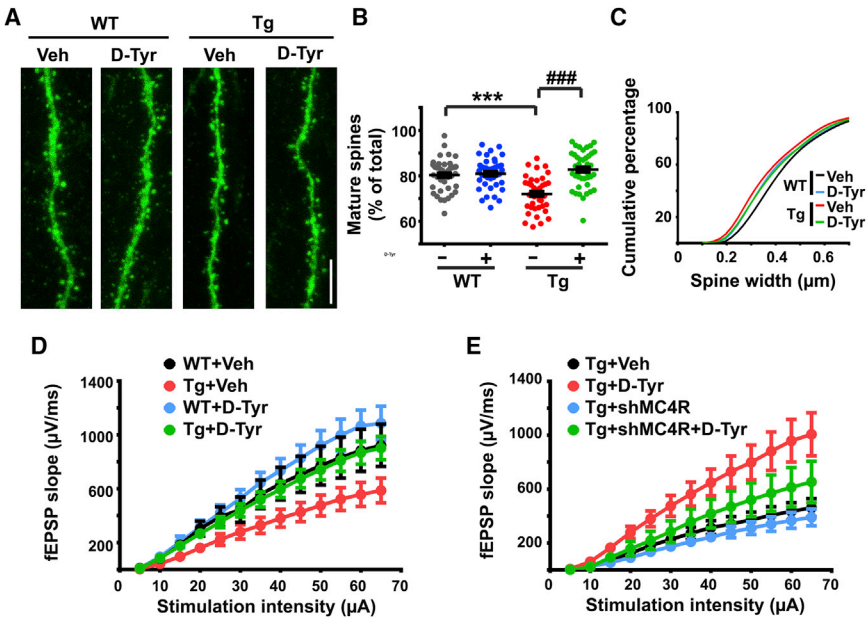

Figure 4. Activation of Hippocampal MC4R Signaling Rescues Defects in Synaptic Morphology and Transmission in APP/PS1 Mice

(A–C) Loss of mature spines in the CA1 region of APP/PS1 mice was reversed by intracerebroventricular (ICV) infusion of D-Tyr for 4 weeks. (A) Representative images of GFP-expressing hippocampal CA1 neurons of 6-month-old mice. Scale bar, 10 μm. (B) Quantification of percentage of mature spines (n = 40 dendrites from 3–5 mice, mean ± SEM). ***$p < 0.001$, Tg versus WT in Con condition; ###$p < 0.001$, Tg D-Tyr versus Tg Con, one-way ANOVA. (C) Cumulative probability analysis of spine width.

(D and E) Stimulation of MC4R reversed hippocampal synaptic transmission impairment in Tg mice, whereas MC4R knockdown attenuated the rescue. Input-output (I/O) curves in response to stimulus in the hippocampal CA1 region of Tg mice with D-Tyr ICV infusion (D) and D-Tyr ICV infusion after shMC4R expression in the CA1 region (E). The input-output curve was measured by averaging the slope of EPSPs against stimulus intensity from 5 to 65 μA (n = 20–30 slices from 10–15 mice).

exacerbated the LTP impairment in 4-month-old APP/PS1 mice, specific activation of Gs signaling, but not Gq, attenuated this impairment (Figures 5E–5H). These results collectively indicate that the activation of hippocampal MC4R/Gs/PKA signaling rescues synaptic plasticity impairment in APP/PS1 mice, thus highlighting an important role of the hippocampal POMC/MC4R circuit in synaptic plasticity impairment during AD progression.

MC4R Protects Hippocampal Synapses from Aβ through cAMP/PKA Signaling

Aβ accumulation in the brain is associated with or possibly induces the dysfunction of synapses and neural networks, contributing to the pathogenesis of AD (Palop and Mucke, 2010). Therefore, we determined whether MC4R activation rescues Aβ-induced hippocampal synaptic impairment. Whereas Aβ treatment reduced SC-CA1 LTP magnitude in acute mouse hippocampal slices, D-Tyr MTII pretreatment prevented the decrease of LTP (Figures 6A and 6B).

Aβ treatment also reduced synaptic transmission, as reflected by the decreased miniature excitatory postsynaptic current (mEPSC) frequency and amplitude in cultured rat hippocampal neurons; meanwhile, co-treatment with D-Tyr MTII abolished these reductions (Figures 6C–6E). MC4R stimulation activates adenylyl cyclase through Gs, which subsequently increases intracellular cAMP levels and enhances downstream effectors including PKA and exchange protein directly activated by cAMP 2 (EPAC) (Balthasar et al., 2005). Accordingly, increasing cAMP levels by co-treatment with forskolin, an activator of adenylyl cyclase, rescued the Aβ-induced reductions of mEPSC frequency and amplitude in hippocampal neurons, whereas the EPAC2 activator 8-4-chlorophenylthio- adenosine 3':5'-cyclic monophosphate (8 CP-cAMP) did not (Figures 6F–6H). Furthermore, the PKA inhibitor H89 abolished the D-Tyr MTII-mediated rescue of the Aβ-induced reduction of mEPSC (Figures 6I–6K). These results collectively suggest that activation of the MC4R/cAMP/PKA signaling pathway protects hippocampal neurons from or reverses Aβ-triggered synaptic impairment. Furthermore, the results suggest that MC4R activation alleviates Aβ-induced synaptic dysfunctions, as evidenced by the restoration of normal synaptic transmission and rescue of synaptic plasticity impairment.

MC4R Exerts Beneficial Effects in Hippocampal Neurons via CREB Activation

CREB, a transcription factor and cellular target of PKA signaling, is essential for memory formation and retention, as well as neuronal survival. Downregulation of CREB signaling is implicated in the pathology of AD (Mantamadiotis et al., 2002; Pugazhenthi et al., 2011). Acute mouse hippocampal slices treated with Aβ, as well as slices from APP/PS1 mouse brains, exhibited reduced CREB activation, as demonstrated by the decreased phosphorylation of CREB at Ser133 (Figure 7A–7D). Meanwhile, D-Tyr MTII treatment restored the CREB signaling in both conditions (Figure 7A–7D), indicating that MC4R mediates the rescue of synaptic functions in APP/PS1 mice probably through the activation of CREB signaling.

Next, we examined whether CREB signaling is required for the MC4R-mediated rescue of synaptic functions. Overexpression of the two dominant-negative CREB mutants, i.e., S133A-CREB (a phosphorylation mutant) and killer CREB (kCREB) (a DNA-binding mutant) (Sarkar et al., 2007), in cultured hippocampal neurons abolished the D-Tyr MTII-mediated rescue of Aβ-induced reduction of mEPSC (Figures 7E–7G). Thus, the results indicate that PKA-dependent activation of CREB and its transcriptional activity are required for the MC4R-mediated protective effect at the hippocampal synapses.

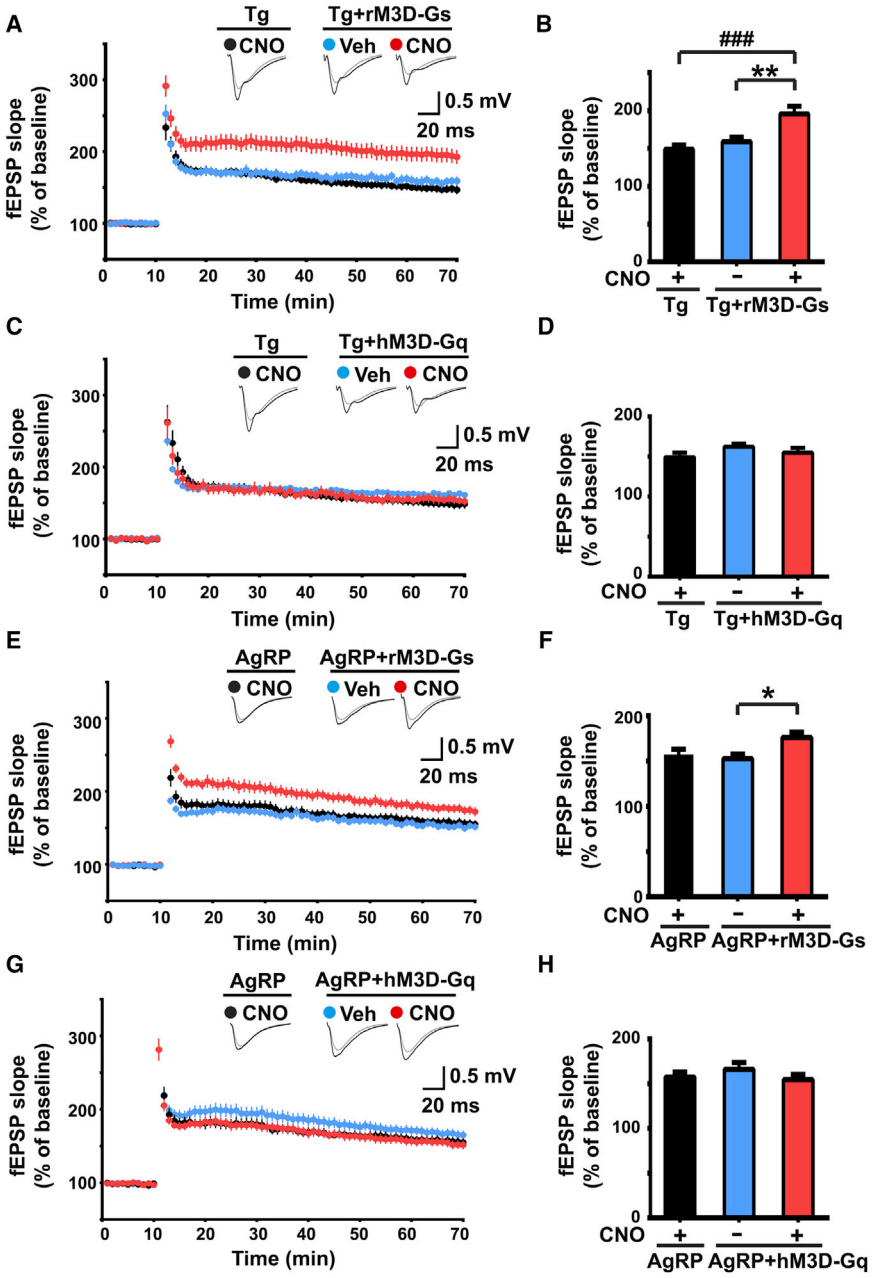

Figure 5. Activation of MC4R-Coupled Gs Signaling Rescues Hippocampal LTP Impairment in APP/PS1 Mice

(A–D) Activation of hippocampal Gs, but not Gq, signaling reversed LTP impairment in 6-month-old Tg mice. (E–H) Activation of hippocampal Gs, but not Gq, signaling reversed the LTP impairment induced by AgRP overexpression in the hippocampus of 4-month-old Tg mice. (A, C, E, and G) LTP in the CA1 of the Schaffer-collateral pathway was induced by two trains of HFS. (B, D, F, and H) Quantification of mean fEPSP slopes as averaged in the last 10 min of the recording after LTP induction (mean ± SEM). (B) $^{**}p < 0.01$, rM3D-Gs CNO versus rM3D-Gs Veh in Tg mice; $^{###}p < 0.001$, rM3D-Gs CNO versus GFP CNO in Tg mice, one-way ANOVA with the Kruskal-Wallis test. (F) $^{*}p < 0.05$, AgRP + rM3D-Gs CNO versus AgRP + rM3D-Gs Veh in Tg mice, one-way ANOVA with the Kruskal-Wallis test. (D and H) Results are not significant.

DISCUSSION

This study revealed the presence of POMC neurons, which secrete POMC-derived peptides upon neuronal activity stimulation, in the hippocampal CA3 area. Moreover, activation of MC4R in the postsynaptic pyramidal neurons in the CA1 region results in PKA-dependent postsynaptic potentiation, ultimately enhancing synaptic plasticity. Dysfunction of this hippocampal POMC/MC4R circuit leads to synaptic plasticity impairment in an AD mouse model. Together with the previous report that POMC/α-MSH is reduced in the CSF and temporal lobe of human AD patients (Catania et al., 2000), our findings suggest that perturbation of the hippocampal POMC/MC4R pathway might, at least in part, contribute to the observed synaptic deficits. Importantly, the results of the present study reveal a molecular target for the disease, wherein the specific activation of MC4R by agonist delivery or replenishment in POMC neurons rescues the LTP impairment in APP/PS1 mice.

In the hippocampus, information signals are modulated by various locally derived neuropeptides, forming the ligand-receptor system among different subregions. The MC4R-dependent modulation of synaptic plasticity is precisely controlled by the accessibility and release of α-MSH. Our study reveals that only a small population of POMC cells is present in the hippocampal CA3 region; nonetheless, their activation is sufficient to contribute to α-MSH secretion in the CA1, subsequently regulating the synaptic functions within the Schaffer-collateral pathway via MC4R activation. Neuropeptides are packaged in large dense-core vesicles and released only under strong neuronal discharge (Zhao et al., 2011). Thus, α-MSH release is believed to be triggered when there are strong inputs into the CA3 and not by basal neuronal activity. Indeed, it is possible that POMC neurons in the CA3 receive multiple inputs including the perforant pathway from the medial and lateral entorhinal cortex (EC), reciprocal connections with the septum, mossy fiber inputs from the DG, and its own outputs fed back as inputs via the recurrent collaterals (Kesner, 2013). However, given that POMC neurons are not evenly distributed in the CA3 region but are mainly localized at the anterior and medial hippocampus, the POMC circuit may not be a general intrinsic circuit within the

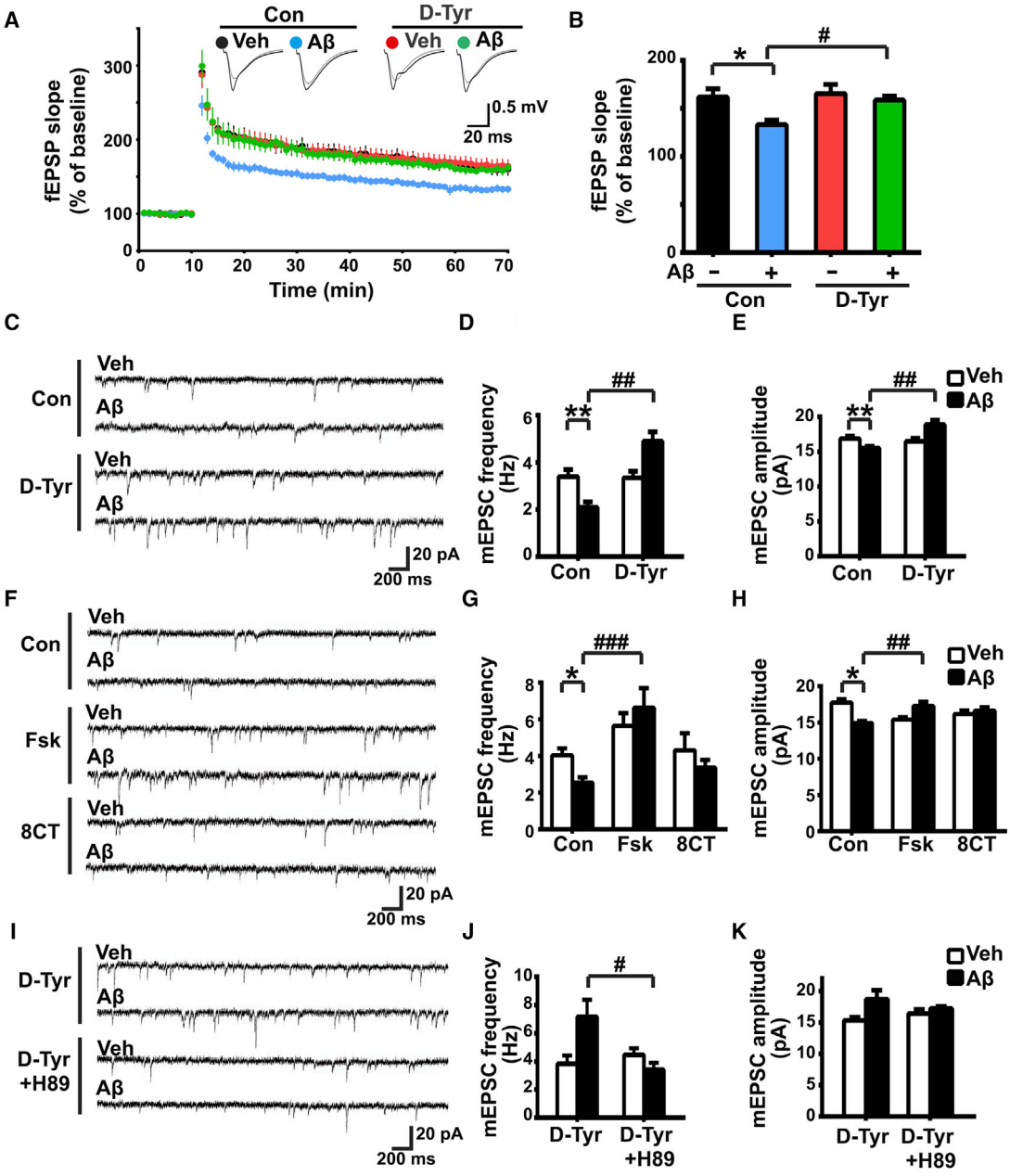

Figure 6. MC4R Signaling Rescues Oligomeric Aβ-Induced Synaptic Dysfunctions in Hippocampal Neurons via the cAMP-PKA Pathway

(A and B) Activation of MC4R signaling rescued Aβ-induced hippocampal LTP impairment. Acute hippocampal slices were treated with Aβ in the presence of D-Tyr for 2 hr. LTP in the CA1 region of the Schaffer-collateral pathway was subsequently induced by two trains of HFS. (A) Summary plot of normalized fEPSP slope measurement. (B) Quantification of mean fEPSP slopes as averaged in the last 10 min of the recording after LTP induction (mean ± SEM). *$p < 0.05$, Aβ versus Veh; #$p < 0.05$, D-Tyr Aβ versus control (Con) Aβ, one-way ANOVA with the Bonferroni post hoc test.

(C–K) Activation of MC4R/cAMP/PKA signaling abolished the Aβ-induced reduction of spontaneous neurotransmission in cultured hippocampus neurons. (C–H) Co-treatment with D-Tyr or forskolin (Fsk), but not 8CT-cAMP (8CT), rescued the Aβ-induced reduction of miniature excitatory postsynaptic current (mEPSC). (I–K) The PKA inhibitor H89 abolished the D-Tyr-stimulated rescue of Aβ-induced reduction of mEPSC. Cultured hippocampal neurons were treated with D-Tyr or D-Tyr + H89 in the presence of Aβ as indicated. (C, F, and I) Representative mEPSC traces from Aβ-stimulated neurons under different treatments. Quantification of frequency (D, G, and J) and amplitude (E, H, and K) of mEPSCs (mean ± SEM). *$p < 0.05$; **$p < 0.01$ versus Veh in Con; #$p < 0.05$; ##$p < 0.01$; ###$p < 0.001$ versus Aβ in Con (or Aβ in D-Tyr for J); one-way ANOVA with the Kruskal-Wallis test.

hippocampus that secretes α-MSH and non-selectively enhances synaptic plasticity in the hippocampus. Besides the intrinsic inputs, POMC neurons can also be under the control of some extrinsic afferents, which may send information to the hippocampus. Such information can be integrated and strengthened through the activation of the hippocampal POMC/MC4R

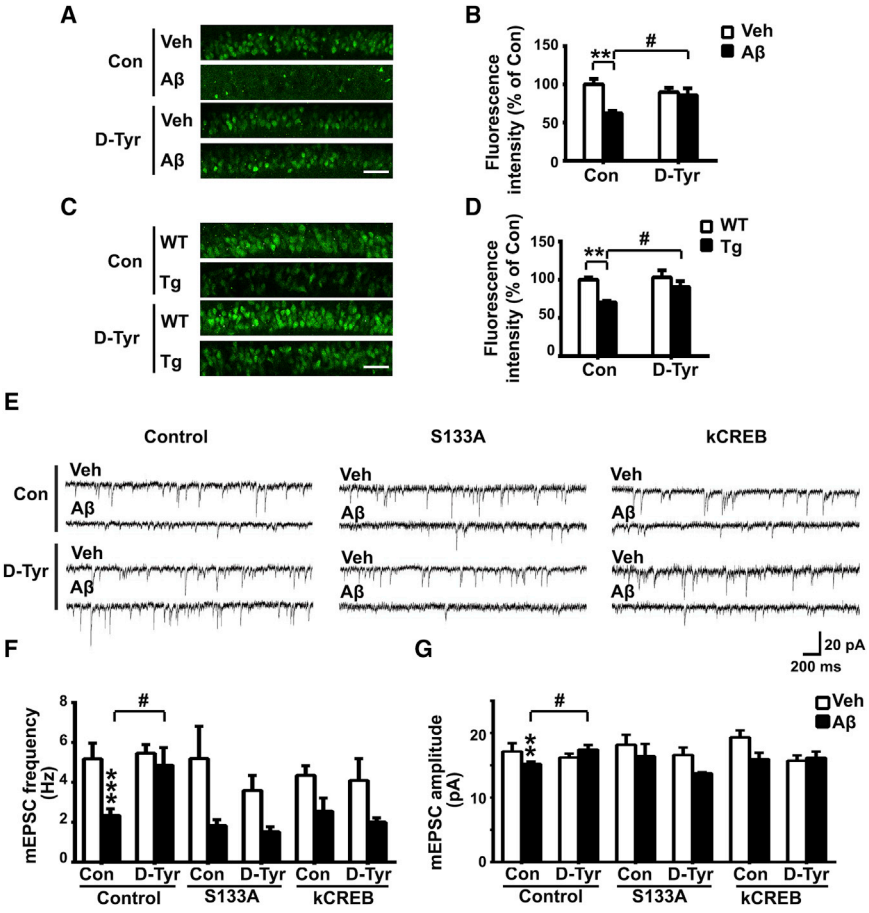

Figure 7. Activation of MC4R Signaling Rescues Synaptic Dysfunctions via CREB Signaling in APP/PS1 Mice

(A–D) MC4R activation restored the high-potassium-stimulated increase of CREB phosphorylation in acute hippocampal slices incubated with Aβ (A and B) or slices from Tg mice (C and D). (A and C) CREB phosphorylated at Ser133 (pCREB) staining in the CA1 pyramidal cell layer. (B and D) Quantification of fluorescence intensity in the CA1 pyramidal cell layer (mean ± SEM; n = 6–10 slices from 3–5 mice). (B) $^{**}p < 0.01$, Aβ versus Veh in control (Con); $^{\#}p < 0.05$, Aβ + D-Tyr versus Aβ; one-way ANOVA with the Kruskal-Wallis test. (D) $^{**}p < 0.01$, Tg versus WT in Con; $^{\#}p < 0.05$, Tg + D-Tyr versus Tg; one-way ANOVA with the Kruskal-Wallis test.

(E–G) The expression of two dominate-negative CREB mutants (S133A CREB and kCREB) abolished the D-Tyr-stimulated rescue of the Aβ-induced reduction of mEPSC in cultured hippocampal neurons. (E) Representative mEPSC traces from Aβ-stimulated neurons under different treatments. Quantification of frequency (F) and amplitude (G) of mEPSCs (mean ± SEM). (F) $^{***}p < 0.001$, Aβ versus Veh in Con; $^{\#}p < 0.05$, Aβ + D-Tyr versus Aβ; (G) $^{**}p < 0.01$, Aβ versus Veh in Con; $^{\#}p < 0.05$, Aβ + D-Tyr versus Aβ; one-way ANOVA with the Bonferroni post hoc test.

circuit. Thus, it would be interesting to know whether the POMC circuit contributes to communication between intra- and extra-hippocampal networks.

Although synaptic plasticity at SC-CA1 synapses is vulnerable in AD (Mattson and Magnus, 2006), we demonstrated that attenuation of the hippocampal POMC/MC4R circuit may contribute to this impaired synaptic plasticity during disease progression. It is important to examine the underlying cellular mechanisms contributing to the deficit of the hippocampal POMC circuit in AD. There are three potential mechanisms. First, decreased *Pomc* transcript levels in the mouse hippocampus upon Aβ treatment or in AD model mice may reflect the loss of hippocampal POMC neurons and contribute to decreased α-MSH secretion. Interestingly, Aβ has been reported to regulate the transcription of neuromodulators in human brain slices (Sebollela et al., 2012). Second, the activity of POMC neurons might be attenuated, resulting in reduced α-MSH secretion during AD progression. The POMC cells in the hypothalamus are silenced by mechanistic target of rapamycin (mTOR) signaling during aging (Yang et al., 2012), and Aβ is reported to induce mTOR hyperactivity (Bové et al., 2011). Therefore, it would be of interest to examine whether the reduced activity of hippocampal POMC cells can be regulated by mTOR signaling in a similar manner. Third, the loss of external input may contribute to the reduced activity of the POMC cells in the hippocampus. The CA3 receives inputs from different brain regions including intrinsic inputs from the DG/CA3 and extrinsic projections from the EC, septum, and basal forebrain (Kesner, 2013; Le Duigou et al., 2014). Interestingly, like the hippocampus, the EC and basal forebrain are highly vulnerable and suffer damage in the early stage of AD (Saxena and Caroni, 2011). Therefore, the hippocampal POMC circuit may connect different brain regions, and dysfunctions of this circuit might be associated with the "spread" of the circuitry malfunctions from vulnerable brain regions (e.g., the EC) to the hippocampus, which ultimately contributes to the global synaptic deficits in AD.

Reversing synaptic dysfunctions is a potential therapeutic strategy to counteract cognitive decline in AD (Selkoe, 2002). Here, we report that stimulation of the hippocampal POMC/MC4R circuit rescues synaptic impairment through the activation of Gs/cAMP/PKA signaling. Similar to MC4R, activation of other Gs-coupled receptors such as β_2-adrenergic receptor prevents Aβ-induced hippocampal LTP impairment (Li et al., 2013). Furthermore, the specific activation of Gs signaling in MC4R-expressing neurons reverses synaptic impairment, suggesting that activation of Gs-coupled receptor signaling alleviates synaptic dysfunctions in AD. Understanding the involvement of specific G-protein-coupled receptors in mediating synaptic dysfunction in AD may aid the development of potential therapeutic strategies. Accordingly, systemic administration of G-protein-coupled receptor agonists, particularly MC4R agonists, exerts a beneficial effect (Giuliani et al., 2014; Ma and McLaurin, 2014). However, the nonselective activation of melanocortin receptors in

the brain may cause various side effects such as anorexia (Barsh and Schwartz, 2002). Thus, the results of our study provide a foundation for an alternative approach to AD treatment, i.e., protecting or preserving POMC neurons in the hippocampus may be more effective than merely administering receptor agonists. Furthermore, although MC4R activation reverses synaptic plasticity impairment in AD, MC4R basal activation must be maintained to prevent the development of synaptic deficits in the hippocampus. Blockade of hippocampal MC4R activity triggers early synaptic impairment in AD mouse models (Figure 2). Thus, identifying ways to replenish the stores of POMC-derived peptides and maintaining MC4R activation is critical for alleviating hippocampal synaptic plasticity impairment. Hence, the POMC/MC4R circuit is a potential therapeutic target for AD-associated cognitive dysfunctions.

EXPERIMENTAL PROCEDURES

Chemicals, Antibodies, and Animals

The details of chemicals and antibodies are described in the Supplemental Experimental Procedures.

The APP/PS1 double-transgenic mice were generated by incorporating a human/murine APP construct bearing the Swedish double mutation and the exon-9-deleted *PSEN1* mutation (*APPswe* + *PSEN1/dE9*) (Jacobsen et al., 2006). *Pomc-Cre* mice have Cre recombinase cDNA inserted at the first ATG transcription start site, ablating the first 30 bp of the *Pomc* coding sequence (McHugh et al., 2007). *Mc4r*^{tb} mice have a *loxP*-flanked transcriptional blocking (*loxTB*) sequence that prevents transcription and translation from the endogenous gene (Balthasar et al., 2005). All the transgenic mice were obtained from Jackson Laboratory. Mouse genotype was confirmed by PCR analysis of tail biopsies. Four to five mice of the same sex were housed per cage with a 12-hr light-dark cycle, as well as food and water ad libitum. Sample sizes were primarily chosen on the basis of experience with similar types of experiments. All animal procedures were conducted in accordance with the Guidelines of the Animal Care Facility of Hong Kong University of Science and Technology (HKUST) and approved by the Animal Ethics Committee of HKUST.

Virus Preparation, Oligomeric Aβ Preparation and Administration, Real-Time PCR, Immunohistochemical Analysis, and Confocal Microscopy

The details of the procedures for virus preparation, oligomeric Aβ preparation and administration, real-time PCR, immunohistochemical analysis, and confocal microscopy are described in the Supplemental Experimental Procedures.

Stereotaxic Surgery

Surgical procedures were performed as described previously (Fu et al., 2014). In brief, animals were anesthetized with 2% isoflurane and placed in a stereotaxic head frame on a heat pad. Ophthalmic ointment was applied to the eyes to prevent drying. A midline incision was made down the scalp, and a craniotomy was performed with a dental drill. A 10-μL NanoFil Hamilton syringe (WPI) with a 33-gauge beveled metal needle was used to infuse virus with a microsyringe pump and its controller (53311; Stoelting Company). Virus was infused at 100–150 nL/min. After infusion, the needle was kept at the injection site for 10 min and then withdrawn slowly. All stereotaxic coordinates are relative to the bregma. The incision was closed with sutures, and the animals were subcutaneously injected with antibiotics before recovery under a heat lamp. The details of viral injection are described in the Supplemental Information (Table S1).

For osmotic pump infusions, 5-month-old AD transgenic mice were implanted with Alzet mini-osmotic pumps (model 1004) set at 0.11 μL/hr for 28 days. The pumps were loaded with either drug or vehicle solvent in artificial cerebrospinal fluid (aCSF). D-Tyr MTII (D-Tyr), MCL 0020, or HS024 was administered at 2.4, 2.0, and 0.2 nmol/day per mouse, respectively. The mini-osmotic pumps were adjusted intracerebroventricularly in the right hemisphere.

Tissue Preparation and Microdissection

Adult male C57BL/6J mice (~3 months old) were anesthetized, and their brains were quickly removed, frozen in liquid-nitrogen-chilled isopentane, and stored at −80°C. Brains were cut into 14-μm-thick sagittal sections using a cryostat at −16°C. The sections were fixed by 75% ethanol (−20°C) and stained with cresyl violet. The three layers of CA1 and CA3 pyramidal cells, as well as DG granule cells, were isolated from the dorsal parts of the mouse hippocampus (1.0–2.0 mm relative to the bregma) using laser capture microdissection (Leica AS LMD; Leica Microsystems) under a 10× objective with charge-coupled device (CCD) camera. The hippocampal subregions were then lysed in the extraction buffer from NucleoSpin RNA kit and stored at −80°C.

Hippocampal Slice Preparation and Treatment

Mice were anesthetized and subsequently euthanized by decapitation. The brain was immediately resected and soaked in ice-cold 95% O_2/5% CO_2 oxygenated aCSF preparation ([in mM] 124 NaCl, 26 $NaHCO_3$, 10 glucose, 3 KCl, 1.25 $NaHPO_4$, 2 $CaCl_2$, and 2 $MgSO_4$ [pH 7.4, 310 mOsm]). Brain slices (300–500 μm) were prepared using a vibrating tissue slicer (HM650V; Thermo Fisher Scientific) and soaked in oxygenated preparation buffer at 32°C for 2 hr.

For the α-MSH secretion assay, 6-month-old mice were anesthetized, and their brains were cut into 0.5-mm-thick sagittal slices with a vibrating tissue slicer (HM650V; Thermo Fisher Scientific). Hippocampal tissues were then resected and immediately transferred into aCSF and maintained at 34°C. The slices were incubated in 500 μL aCSF for 2 hr and then transferred to aCSF containing high potassium (KCl was switched from 2.5 to 50 mM and NaCl from 126.5 to 78.5 mM to maintain tonicity) or aCSF with 1 μM CNO for 2–4 hr. After treatment, the aCSF was collected and subjected to fluorescence immunoassay for α-MSH (Phoenix Pharmaceuticals) according to the manufacturer's instructions.

For phosphorylated CREB (pCREB) detection, 3-month-old C57 mice or 6-month-old APP/PS1 mice were anesthetized, and their brains were cut into 300-μm-thick sagittal slices and incubated in aCSF with different treatment (1 μM D-Tyr MTII, 500 nM Aβ) at 34°C for 2 hr. The slices were subsequently transferred to aCSF containing high potassium (KCl was switched from 2.5 to 90 mM and NaCl from 126.5 to 38.5 mM to maintain tonicity) for 3 min and returned to the conditional aCSF. One hour after stimulation, the slices were fixed with 4% paraformaldehyde and immunostaining was performed.

Electrophysiology

Rat hippocampal neurons at 16–20 days in vitro were used to measure mEPSCs. The cells were treated with 500 nM Aβ for 24 hr alone or together with different drug combinations as indicated (1 μM D-Tyr MTII, 2 μM forskolin, 5 μM rolipram, and 10 μM H89). Whole-cell patch-clamp recordings were made at room temperature. The external solution comprised (in mM) 110 NaCl, 5 KCl, 2 $CaCl_2$, 0.8 $MgCl_2$, 10 HEPES, and 10 D-glucose (pH 7.4); the internal solution comprised (in mM) 135 $CsCl_2$, 10 HEPES, 2 $MgCl_2$, 4 NaATP, 0.4 guanosine 5'-triphosphate sodium salt hydrate (NaGTP), and 0.5 EGTA (pH 7.2). Picrotoxin (200 μM) was included in the external solution to block GABAergic inhibitory postsynaptic potentials, and tetrodotoxin (0.5 μM) was added to prevent action-potential-evoked EPSCs. Cells were held at −70 mV for mEPSC recordings. Pipette and series resistances were typically 3–5 and 15–20 MΩ, respectively. Only recording epochs in which series and input resistances varied by <10% were analyzed. At least 10 neurons were recorded in each experiment.

For LTP recording, brain slices (300 μm) were prepared and soaked in oxygenated preparation buffer at 32°C for 2 hr. The hippocampal regions were resected and placed on the center of a MED-P210A probe (Panasonic International) with 64 embedded recording sites. The slices were then perfused with oxygenated aCSF at 28°C–32°C. Extracellular field potentials were recorded using a MED64 multichannel recording system, and data were collected from the dendritic layer of area CA1 at a sampling rate of 10 kHz. For each slice, the baseline stimulus intensity was set at the level that elicited ~40% of the maximum fEPSP response as determined from the input-output

curve. The fEPSP responses were recorded for at least 40 min before LTP induction to ensure stability of the response. LTP was induced by two trains of high-frequency stimulation (100 Hz for 1 s delivered 30 s apart). The LTP magnitude was quantified as the percentage change in the fEPSP slope (10%–90%) taken during the 60-min interval after LTP induction.

Quantification and Statistical Analysis

The investigators who collected and analyzed the electrophysiological and staining data were blinded to the mouse genotypes and treatment conditions. Error bars in the figures indicate the SEM. All statistical analyses were performed using GraphPad Prism 6. For biochemical experiments, n designates the number of mouse brains or slice samples per condition; for mEPSC and LTP measurements, n designates the numbers of neurons and slices, respectively. Statistical significance was assessed by Student's t test, or one- or two-way ANOVA where appropriate, followed by the indicated post hoc tests. All experiments were performed at least three times, except where indicated. The level of significance was set at $p < 0.05$.

SUPPLEMENTAL INFORMATION

Supplemental Information includes Supplemental Experimental Procedures, five figures, and one table and can be found with this article online at http://dx.doi.org/10.1016/j.celrep.2016.10.043.

AUTHOR CONTRIBUTIONS

Y.S., M.T., Y.Z., and F.G. conducted the experiments. Y.S., M.T., Y.Z., F.G., A.K.Y.F., and N.Y.I. analyzed the data. Y.S., A.K.Y.F., and N.Y.I. designed the experiments and wrote the paper.

ACKNOWLEDGMENTS

We are grateful to Drs. Karl Deisseroth (Stanford University), Eriika Savontaus (University of Turku), and Roger Adan (University Medical Center Utrecht) for generously providing the expression constructs. We also thank Drs. Edward Boyden (Massachusetts Institute of Technology Media Lab), Tyler Jacks (Massachusetts Institute of Technology), and Domenico Accili (Columbia University Medical Center) for providing expression constructs through Addgene. We thank Dr. Liping Wang (Shenzhen Institutes of Advanced Technology, Chinese Academy of Sciences) for the generation of viruses. We also thank Dr. Yu Chen, Dr. Yuewen Chen, Cara Kwong, Elaine Cheng, and William Chau for their excellent technical assistance; Dr. Wing-Yu Fu for her critical reading of the manuscript; and other members of the N.Y.I. laboratory for many helpful discussions. This study was supported in part by the Research Grants Council of Hong Kong SAR (grants HKUST661013, HKUST16102715, and HKUST16102815), the National Key Basic Research Program of China (grant 2013CB530900), the Health and Medical Research Fund (grant HMRF14SC07), the Hong Kong Research Grants Council Theme-Based Research Scheme (grant T13-607/12R), and the SH Ho Foundation. Y.S. is a recipient of the MSD R&D China Postdoctoral Research Fellowship Award.

Received: October 12, 2015
Revised: July 27, 2016
Accepted: October 13, 2016
Published: November 8, 2016

REFERENCES

Alexander, G.M., Rogan, S.C., Abbas, A.I., Armbruster, B.N., Pei, Y., Allen, J.A., Nonneman, R.J., Hartmann, J., Moy, S.S., Nicolelis, M.A., et al. (2009). Remote control of neuronal activity in transgenic mice expressing evolved G protein-coupled receptors. Neuron *63*, 27–39.

Balthasar, N., Dalgaard, L.T., Lee, C.E., Yu, J., Funahashi, H., Williams, T., Ferreira, M., Tang, V., McGovern, R.A., Kenny, C.D., et al. (2005). Divergence of melanocortin pathways in the control of food intake and energy expenditure. Cell *123*, 493–505.

Banke, T.G., Bowie, D., Lee, H., Huganir, R.L., Schousboe, A., and Traynelis, S.F. (2000). Control of GluR1 AMPA receptor function by cAMP-dependent protein kinase. J. Neurosci. *20*, 89–102.

Barsh, G.S., and Schwartz, M.W. (2002). Genetic approaches to studying energy balance: perception and integration. Nat. Rev. Genet. *3*, 589–600.

Beckwith, B.E., Sandman, C.A., Hothersall, D., and Kastin, A.J. (1977). Influence of neonatal injections of alpha-MSH on learning, memory and attention in rats. Physiol. Behav. *18*, 63–71.

Borbély, E., Scheich, B., and Helyes, Z. (2013). Neuropeptides in learning and memory. Neuropeptides *47*, 439–450.

Bové, J., Martínez-Vicente, M., and Vila, M. (2011). Fighting neurodegeneration with rapamycin: mechanistic insights. Nat. Rev. Neurosci. *12*, 437–452.

Catania, A., Airaghi, L., Colombo, G., and Lipton, J.M. (2000). Alpha-melanocyte-stimulating hormone in normal human physiology and disease states. Trends Endocrinol. Metab. *11*, 304–308.

Fu, A.K., Hung, K.W., Huang, H., Gu, S., Shen, Y., Cheng, E.Y., Ip, F.C., Huang, X., Fu, W.Y., and Ip, N.Y. (2014). Blockade of EphA4 signaling ameliorates hippocampal synaptic dysfunctions in mouse models of Alzheimer's disease. Proc. Natl. Acad. Sci. USA *111*, 9959–9964.

Ghamari-Langroudi, M., Digby, G.J., Sebag, J.A., Millhauser, G.L., Palomino, R., Matthews, R., Gillyard, T., Panaro, B.L., Tough, I.R., Cox, H.M., et al. (2015). G-protein-independent coupling of MC4R to Kir7.1 in hypothalamic neurons. Nature *520*, 94–98.

Giuliani, D., Bitto, A., Galantucci, M., Zaffe, D., Ottani, A., Irrera, N., Neri, L., Cavallini, G.M., Altavilla, D., Botticelli, A.R., et al. (2014). Melanocortins protect against progression of Alzheimer's disease in triple-transgenic mice by targeting multiple pathophysiological pathways. Neurobiol. Aging *35*, 537–547.

Guettier, J.M., Gautam, D., Scarselli, M., Ruiz de Azua, I., Li, J.H., Rosemond, E., Ma, X., Gonzalez, F.J., Armbruster, B.N., Lu, H., et al. (2009). A chemical-genetic approach to study G protein regulation of beta cell function in vivo. Proc. Natl. Acad. Sci. USA *106*, 19197–19202.

Jacobsen, J.S., Wu, C.C., Redwine, J.M., Comery, T.A., Arias, R., Bowlby, M., Martone, R., Morrison, J.H., Pangalos, M.N., Reinhart, P.H., and Bloom, F.E. (2006). Early-onset behavioral and synaptic deficits in a mouse model of Alzheimer's disease. Proc. Natl. Acad. Sci. USA *103*, 5161–5166.

Kapogiannis, D., and Mattson, M.P. (2011). Disrupted energy metabolism and neuronal circuit dysfunction in cognitive impairment and Alzheimer's disease. Lancet Neurol. *10*, 187–198.

Kesner, R.P. (2013). A process analysis of the CA3 subregion of the hippocampus. Front. Cell. Neurosci. *7*, 78.

Kishi, T., Aschkenasi, C.J., Lee, C.E., Mountjoy, K.G., Saper, C.B., and Elmquist, J.K. (2003). Expression of melanocortin 4 receptor mRNA in the central nervous system of the rat. J. Comp. Neurol. *457*, 213–235.

La Joie, R., Landeau, B., Perrotin, A., Bejanin, A., Egret, S., Pélerin, A., Mézenge, F., Belliard, S., de La Sayette, V., Eustache, F., et al. (2014). Intrinsic connectivity identifies the hippocampus as a main crossroad between Alzheimer's and semantic dementia-targeted networks. Neuron *81*, 1417–1428.

Larson, M.E., and Lesné, S.E. (2012). Soluble Aβ oligomer production and toxicity. J. Neurochem. *120* (*Suppl 1*), 125–139.

Le Duigou, C., Simonnet, J., Teleñczuk, M.T., Fricker, D., and Miles, R. (2014). Recurrent synapses and circuits in the CA3 region of the hippocampus: an associative network. Front. Cell. Neurosci. *7*, 262.

Lemon, N., and Manahan-Vaughan, D. (2006). Dopamine D1/D5 receptors gate the acquisition of novel information through hippocampal long-term potentiation and long-term depression. J. Neurosci. *26*, 7723–7729.

Li, S., Jin, M., Zhang, D., Yang, T., Koeglsperger, T., Fu, H., and Selkoe, D.J. (2013). Environmental novelty activates β2-adrenergic signaling to prevent the impairment of hippocampal LTP by Aβ oligomers. Neuron *77*, 929–941.

Lin, Y.W., Min, M.Y., Chiu, T.H., and Yang, H.W. (2003). Enhancement of associative long-term potentiation by activation of beta-adrenergic receptors at CA1 synapses in rat hippocampal slices. J. Neurosci. *23*, 4173–4181.

Ma, K., and McLaurin, J. (2014). α-Melanocyte stimulating hormone prevents GABAergic neuronal loss and improves cognitive function in Alzheimer's disease. J. Neurosci. *34*, 6736–6745.

Machado, I., González, P., Schiöth, H.B., Lasaga, M., and Scimonelli, T.N. (2010). α-Melanocyte-stimulating hormone (α-MSH) reverses impairment of memory reconsolidation induced by interleukin-1 beta (IL-1 beta) hippocampal infusions. Peptides *31*, 2141–2144.

Malenka, R.C., and Bear, M.F. (2004). LTP and LTD: an embarrassment of riches. Neuron *44*, 5–21.

Mantamadiotis, T., Lemberger, T., Bleckmann, S.C., Kern, H., Kretz, O., Martin Villalba, A., Tronche, F., Kellendonk, C., Gau, D., Kapfhammer, J., et al. (2002). Disruption of CREB function in brain leads to neurodegeneration. Nat. Genet. *31*, 47–54.

Mattson, M.P., and Magnus, T. (2006). Ageing and neuronal vulnerability. Nat. Rev. Neurosci. *7*, 278–294.

McHugh, T.J., Jones, M.W., Quinn, J.J., Balthasar, N., Coppari, R., Elmquist, J.K., Lowell, B.B., Fanselow, M.S., Wilson, M.A., and Tonegawa, S. (2007). Dentate gyrus NMDA receptors mediate rapid pattern separation in the hippocampal network. Science *317*, 94–99.

Millington, G.W. (2007). The role of proopiomelanocortin (POMC) neurones in feeding behaviour. Nutr. Metab. (Lond.) *4*, 18.

Nusbaum, M.P., and Blitz, D.M. (2012). Neuropeptide modulation of microcircuits. Curr. Opin. Neurobiol. *22*, 592–601.

Ogren, S.O., Kuteeva, E., Elvander-Tottie, E., and Hökfelt, T. (2010). Neuropeptides in learning and memory processes with focus on galanin. Eur. J. Pharmacol. *626*, 9–17.

Palop, J.J., and Mucke, L. (2010). Amyloid-beta-induced neuronal dysfunction in Alzheimer's disease: from synapses toward neural networks. Nat. Neurosci. *13*, 812–818.

Palop, J.J., Chin, J., and Mucke, L. (2006). A network dysfunction perspective on neurodegenerative diseases. Nature *443*, 768–773.

Pugazhenthi, S., Wang, M., Pham, S., Sze, C.I., and Eckman, C.B. (2011). Downregulation of CREB expression in Alzheimer's brain and in Aβ-treated rat hippocampal neurons. Mol. Neurodegener. *6*, 60.

Sandman, C.A., Beckwith, B.E., and Kastin, A.J. (1980). Are learning and attention related to the sequence of amino acids in ACTH/MSH peptides? Peptides *1*, 277–280.

Sarkar, S.A., Gunter, J., Bouchard, R., Reusch, J.E.B., Wiseman, A., Gill, R.G., Hutton, J.C., and Pugazhenthi, S. (2007). Dominant negative mutant forms of the cAMP response element binding protein induce apoptosis and decrease the anti-apoptotic action of growth factors in human islets. Diabetologia *50*, 1649–1659.

Saxena, S., and Caroni, P. (2011). Selective neuronal vulnerability in neurodegenerative diseases: from stressor thresholds to degeneration. Neuron *71*, 35–48.

Scharfman, H.E., and Myers, C.E. (2013). Hilar mossy cells of the dentate gyrus: a historical perspective. Front. Neural Circuit *6*, 106.

Sebollela, A., Freitas-Correa, L., Oliveira, F.F., Paula-Lima, A.C., Saraiva, L.M., Martins, S.M., Mota, L.D., Torres, C., Alves-Leon, S., de Souza, J.M., et al. (2012). Amyloid-β oligomers induce differential gene expression in adult human brain slices. J. Biol. Chem. *287*, 7436–7445.

Selkoe, D.J. (2002). Alzheimer's disease is a synaptic failure. Science *298*, 789–791.

Shen, Y., Fu, W.Y., Cheng, E.Y.L., Fu, A.K.Y., and Ip, N.Y. (2013). Melanocortin-4 receptor regulates hippocampal synaptic plasticity through a protein kinase A-dependent mechanism. J. Neurosci. *33*, 464–472.

Yang, S.B., Tien, A.C., Boddupalli, G., Xu, A.W., Jan, Y.N., and Jan, L.Y. (2012). Rapamycin ameliorates age-dependent obesity associated with increased mTOR signaling in hypothalamic POMC neurons. Neuron *75*, 425–436.

Zhao, B., Wang, H.B., Lu, Y.J., Hu, J.W., Bao, L., and Zhang, X. (2011). Transport of receptors, receptor signaling complexes and ion channels via neuropeptide-secretory vesicles. Cell Res. *21*, 741–753.

Cell Reports, Volume *17*

Supplemental Information

Stimulation of the Hippocampal POMC/MC4R Circuit Alleviates Synaptic Plasticity Impairment in an Alzheimer's Disease Model

Yang Shen, Min Tian, Yuqiong Zheng, Fei Gong, Amy K.Y. Fu, and Nancy Y. Ip

Figure S1

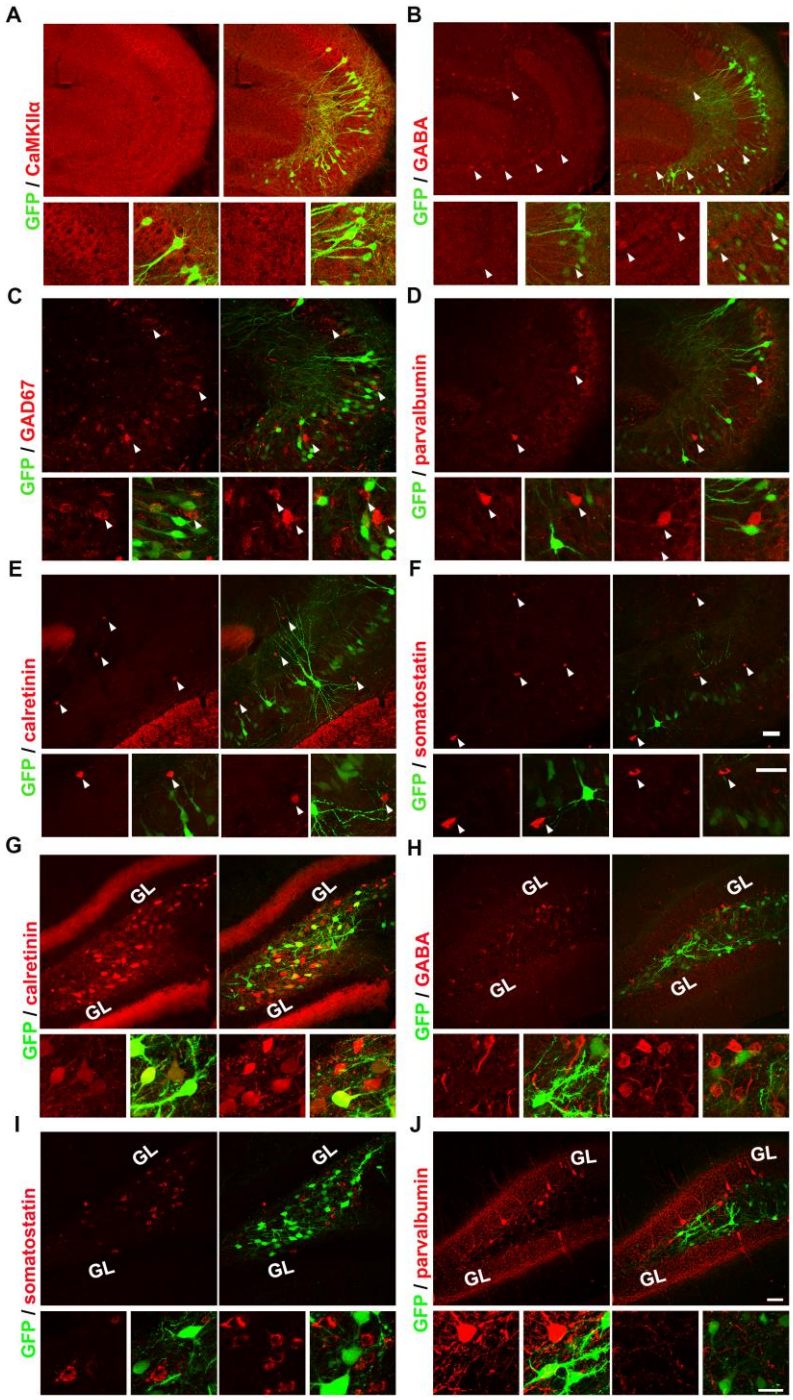

Figure S1, related to Figure 1. Characterization of CA3 POMC cells in the mouse hippocampus.

(A-F) Molecular and anatomical characterization of POMC-positive cells in the CA3. Representative images showing co-labeling of GFP cells with CaMKIIα, GABA, GAD67, parvalbumin, calretinin and

somatostatin. Scale bars: top, 100 μm; bottom, 50 μm. Arrows: neurons labelled with specific markers. (G–J) Molecular and anatomical definitions of hilar POMC-positive cells. Representative images showing GFP expression and co-staining of interneuron markers: calretinin, GABA, somatostatin, and parvalbumin. GL (granule cell layers); scale bars: top, 10 μm; bottom, 50 μm.

Figure S2

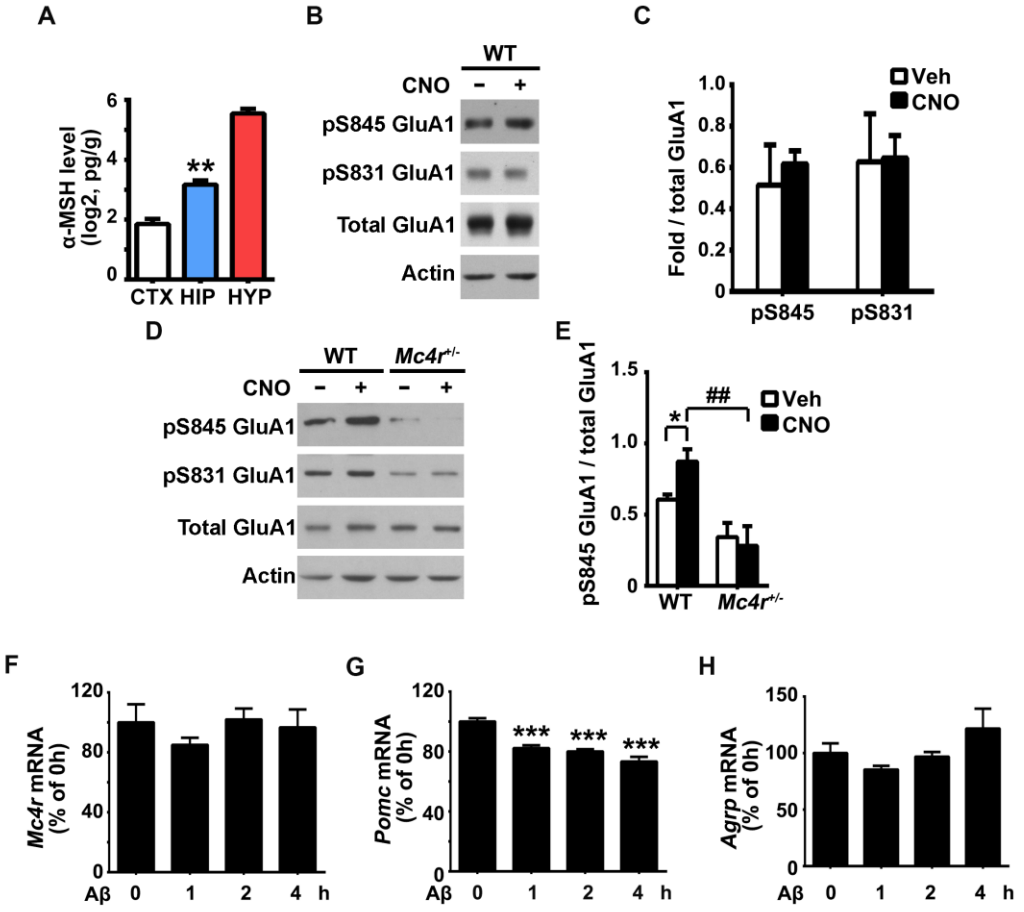

Figure S2, related to Figure 1. Characterization of hippocampal POMC/MC4R signaling in the mouse hippocampus. (A) Basal levels of α-MSH in the adult mouse cortex, hippocampus, and hypothalamus. α-MSH in different tissues was quantified by ELISA (n = 3 mice; $^{**}p < 0.01$, HIP vs. CTX, Student's *t*-test). (B and C) Hilar POMC cell activation did not affect pS845 levels of GluA1 in the CA1. (C) Quantification of band intensity (pS845 GluA1 or pS831 GluA1 normalized to the total GluA1; $n = 4$ experiments). (D and E) Hippocampal POMC cell firing enhanced pS845 GluA1 in the CA1, which was abolished in *Mc4r*$^{+/-}$ mouse hippocampus as shown by western blot analysis. (E) Quantification of band intensity (pS845 GluA1/total GluA1; $^{*}p < 0.05$, CNO vs. Veh, Student's *t*-test; $^{\#\#}p < 0.01$ *Mc4r*$^{+/-}$ +CNO vs WT+CNO, one-way ANOVA with Bonferroni test.; $n = 3$ experiments). (F-H) The hippocampal POMC/MC4R circuit is sensitive to Aβ treatment. Acute mouse hippocampal slices were treated with Aβ for 0–4 h. Quantification of mRNA levels of *Mc4r* (F), *Pomc* (G), and *Agrp* (H).

Figure S3

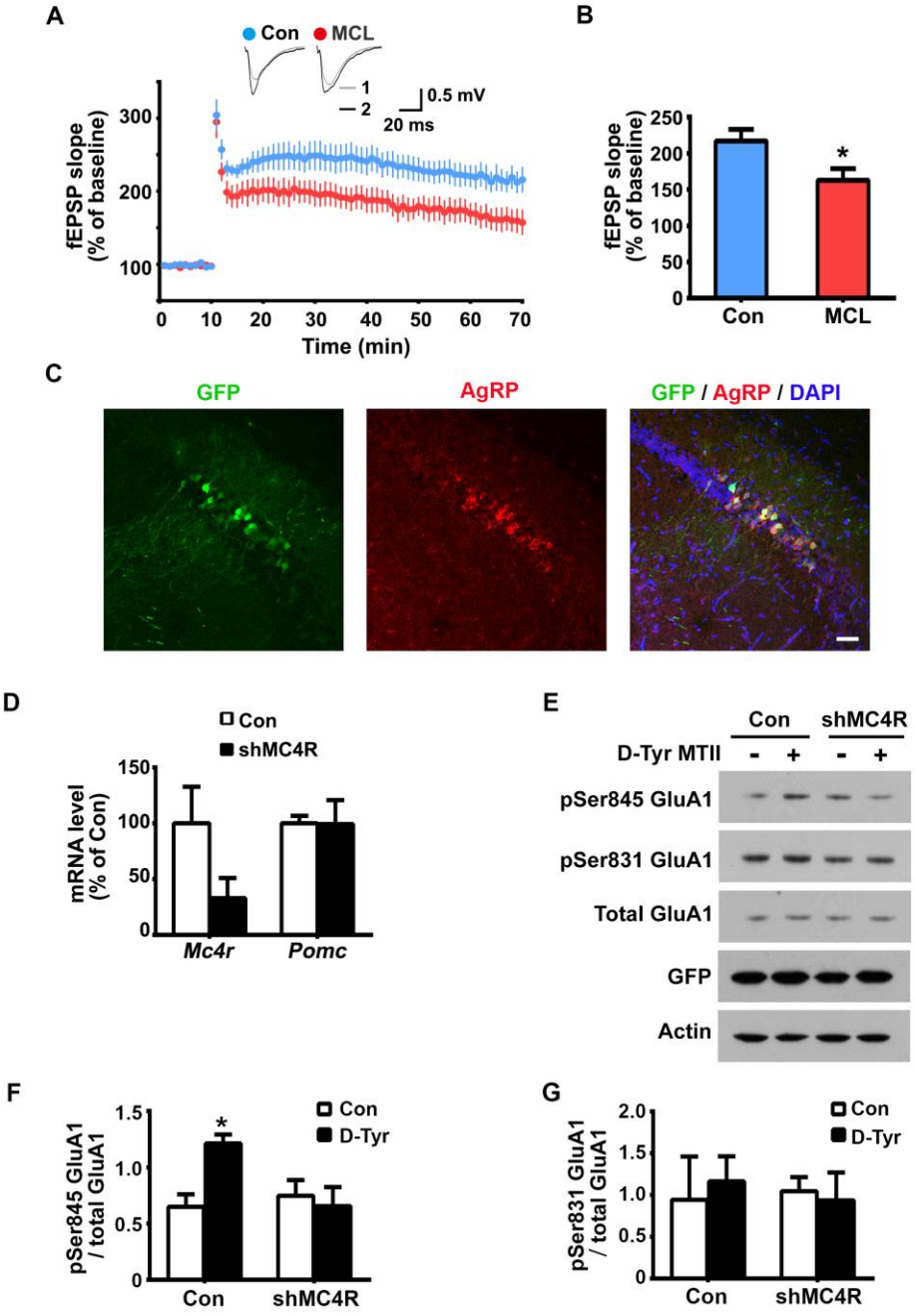

Figure S3, related to Figure 2. MC4R mediates the postsynaptic action of D-Tyr MTII and regulates hippocampal synaptic plasticity. (A and B) Intracerebroventricular infusion of MCL 0020 (MCL) resulted in early long-term potentiation (LTP) impairment in APP/PS1 mice. (A) LTP in the

CA1 of the Schaffer collateral pathway was induced by 2 trains of high-frequency stimulation. (B) Quantification of mean field excitatory postsynaptic potential slopes as averaged in the last 10 min of the recording after LTP induction (mean ± SEM, *$p < 0.05$ MCL vs. Con; Student's *t*-test). (C) Virus-mediated overexpression of AgRP in the mouse hippocampus (co-injection of GFP-expressing AAV labeled the infected cells); scale bar = 100 μm. (D–G) Virus-mediated MC4R knockdown abolished the D-Tyr MTII-induced phosphorylation of GluA1 at Ser845 in hippocampal neurons. Cultured mouse hippocampal neurons (14 days *in vitro* [DIV]) were infected with HIV-shMC4R and examined at 21 DIV. (D) HIV-shMC4R infection significantly decreased *Mc4r* mRNA level but did not change *Pomc* mRNA level. (E–G) The shMC4R knockdown hippocampal neurons were treated with D-Tyr MTII for 2 h and then subjected to western blot analysis. (E) Representative image. (F and G) Quantitative analysis (*$p < 0.05$, D-Tyr MTII vs. Con; two-way ANOVA).

Figure S4

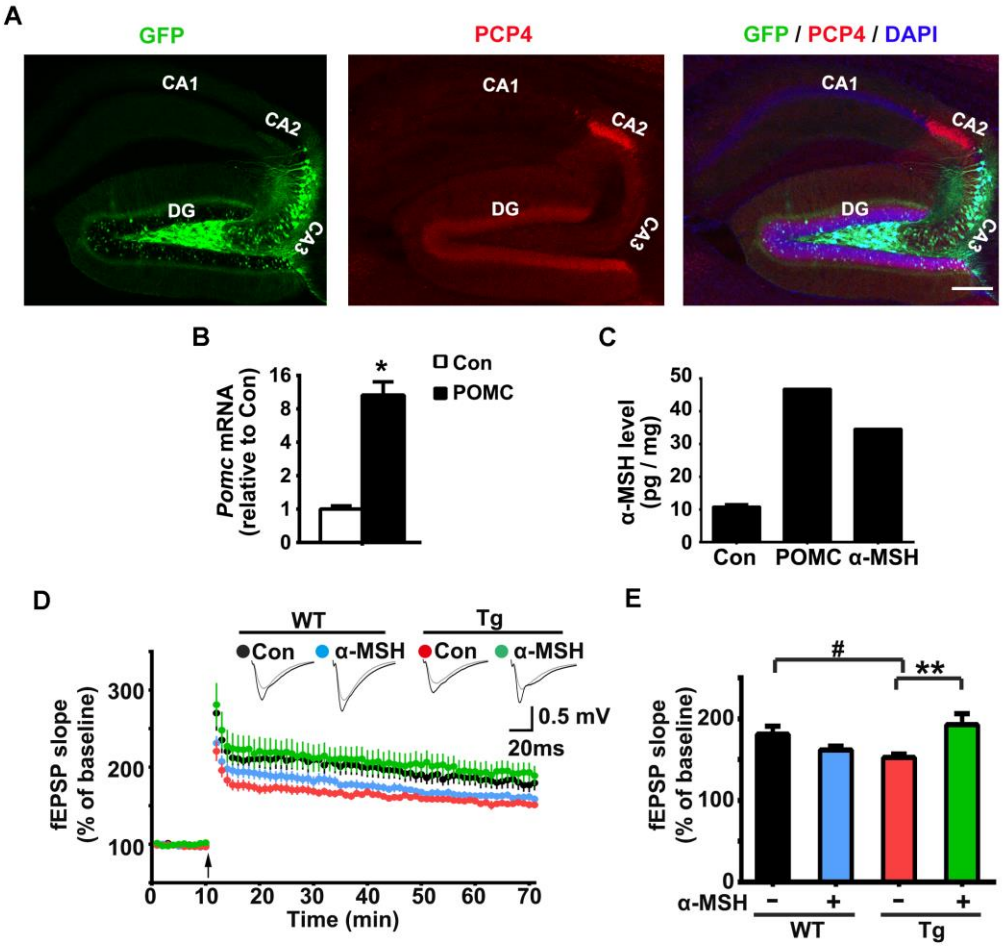

Figure S4, related to Figure 3. Activation of POMC/MC4R in the mouse hippocampus. (A) Labeling of POMC cells in the mouse hippocampus. AAV9-Pomc-Cre and AAV9-FLEX-EGFP were co-injected into the mouse brains. GFP (green) and PCP4 staining (red) label the infected cells and CA2 cells, respectively. Scale bar = 100 μm. (B and C) Overexpression of AAV-POMC/α-MSH in the mouse hippocampus. (B) *Pomc* mRNA levels in the mouse hippocampus 2 weeks after POMC -expressing AAV injection. The data are presented as the relative ratio of mRNA versus that of GAPDH (mean ± SEM, *$p < 0.05$ vs. Con; Student's *t*-test). (C) α-MSH levels in the hippocampal slices prepared from mice with POMC and α-MSH overexpression. (D and E) Overexpression of α-MSH specifically in hippocampal POMC cells significantly reversed CA1 LTP impairment in APP/PS1 mice. (D) Summary plot of normalized fEPSP slope measurement (mean ± SEM). (E) Quantification of mean fEPSP slopes as averaged in the last 10 min of the recording after LTP induction. (mean ± SEM; $^{\#}p < 0.05$, Tg Con vs. WT Con, **$p < 0.01$, Tg α-MSH vs. Tg Con, one-way ANOVA with Bonferroni test.)

Figure S5

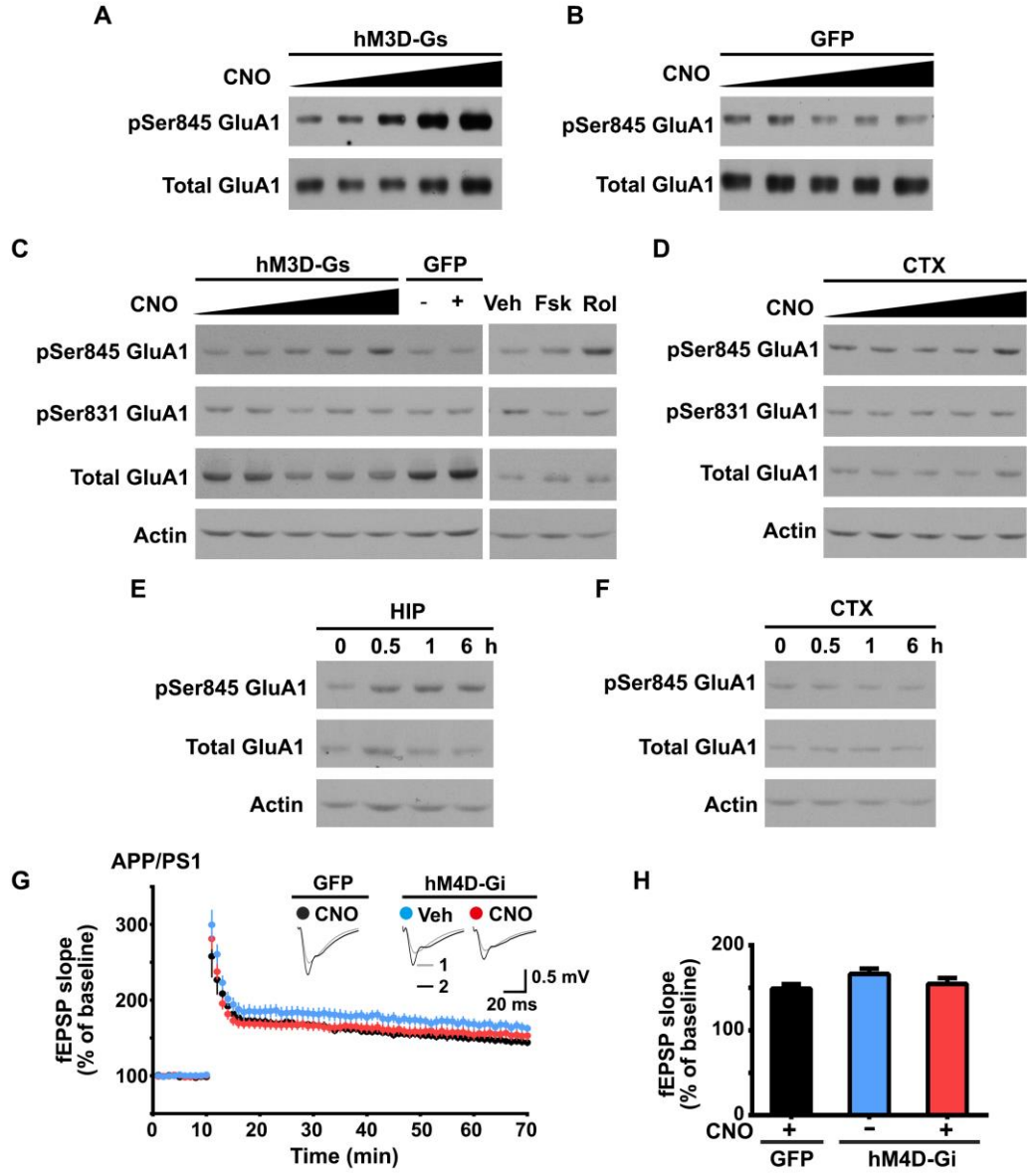

Figure S5, related to Figure 5. Activation of hippocampal Gs signaling increases pSer845 GluA1 levels. (A-F) rM3D-Gs activation increased pSer845 GluA1 level in the mouse hippocampus. (A and B) Acute hippocampal slices from *AAV5-rM3D-Gs* injected mice were treated with clozapine-*N*-oxide (CNO) for 1 h. CNO treatment increased pSer845 GluA1 level in rM3D-Gs–expressing slices in a dose-dependent manner (A) but not in slices from mice expressing GFP (B). (C and D) CNO injection increased pSer845 GluA1 level in the mouse hippocampus expressing rM3D-Gs in a dose-dependent

manner (C) but not in the cortices that did not express rM3D-Gs (D). Forskolin (Fsk) and rolipram (Rol) were used as positive controls. (E and F) Time course of pSer845 GluA1 increase in the hippocampus (E) and cortex (F) after CNO injection. (G and H) Activation of hippocampal Gi signaling failed to rescue LTP impairment in 6-month-old APP/PS1 mice. (G) LTP in the CA1 of the Schaffer collateral pathway was induced by 2 trains of high-frequency stimulation. (H) Quantification of mean field excitatory postsynaptic potential slopes as averaged in the last 10 min of the recording after LTP induction.

Table S1, Stereotaxic coordinates for virus injection, related to Stereotaxic surgery in Experimental Procedures.

SUPPLEMENTAL EXPERIMENTAL PROCEDURES

Chemicals and antibodies

Anti-pSer845 GluA1 (p1160-845) and anti-GluA1 antibodies (895-GluR1) were purchased from PhosphoSolutions; anti-pSer831 GluA1 (p1160-831), anti-parvalbumin (MAB1572), and anti-somatostatin antibodies (MAB354) were purchased from Millipore; anti-GFP antibodies (A-11120) were purchased from Life Technologies; anti-Purkinje cell protein 4 (PCP4; HPA005792), anti-calretinin (C7479), and anti-GABA (#2052) antibodies were purchased from Sigma-Aldrich; anti-pCREB S133 (87G3, #9198) was purchased from Cell Signaling Technology. The D-Tyr MTII (D-Tyr), α-melanocyte-stimulating hormone (MSH) assay kit, and AgRP assay kit were from Phoenix Pharmaceuticals. H89 (*N*-[2-(*p*-bromocinnamylamino)ethyl]-5-isoquinolinesulfonamide dihydrochloride hydrate), 8 CP-cAMP, clozapine-*N*-oxide (CNO), MCL0020, and HS024 were purchased from Tocris, and Aβ monomer was from rPeptide.

Real time-PCR

Total RNA was prepared using RNeasy columns (Qiagen) according to the manufacturer's instructions. Single-stranded cDNA was synthesized using SuperScript II Reverse Transcriptase (Invitrogen) and random hexamers. Real-time PCR was performed with SYBR Green-based reagents (SYBR Green PCR kit; Qiagen) using a 7500 Fast Real-Time PCR System (Applied Biosystems). The mRNA expression was normalized to that of *Gapdh*. Data were obtained from 3 independent experiments.

The following primers used for real-time PCR: mouse *Mc4r*,

5′-GCGTTTCGAATGGGTCGGAAACCA-3′ and 5′-CCGCAATGGAAAGCAGGCTGCAA-3′; mouse *Pomc*, 5′-CTGGAGCAACCCGCCCAAGGA-3′ and 5′-GCGCGTTCTTGATGATGGCGTTCT-3′; mouse *Agrp*, 5′-CTCGTTCTCCGCGTCGCTGTG-3′ and 5′-ACCCAGCTTGCGGCAGTAGCA-3′; mouse *Gapdh* 5′-TGCACCACCAACTGCTTAGC-3′ and 5′-GCCATGGACTGTGGTCATGAG-3′.

Viral constructs

The following target sequence was used to generate the lentiviral shRNA construct: mouse *Mc4r* shRNA, 5′-GAACAAGAACCTGCACTCA-3′. *Mc4r* shRNA oligonucleotides were subcloned into the FUGW vector. *Pomc* shRNA oligonucleotides were subcloned into the p*Sico* vector (a gift from Tyler Jacks, Massachusetts Institute of Technology; Addgene plasmid #11578).

For the *Pomc-Cre* construct, the *Pomc* promoter sequence was amplified from *Pomc-pGL3* (a gift from Domenico Accili, Columbia University Medical Center; Addgene plasmid #17553), and the Cre cDNA sequence was amplified from Cre transgenic mouse DNA. Corresponding sequences were subcloned into the *AAV-CaMKIIa-eYFP* plasmid (a gift from Karl Deisseroth, Stanford University). For *AAV-EF1a-DIO-a-MSH* and *AAV-EF1a-DIO-POMC* constructs, α-MSH cDNA together with a leader sequence were amplified from *WPI-a-MSH-EGFP* (a gift from Eriika Savontaus, University of Turku). *Pomc* cDNA was purchased from the Mammalian Gene Collection (GE Healthcare; MMM1013-202842398). α-MSH or *Pomc* cDNA sequences were subcloned into the backbone of *AAV-EF1a-DIO-EYFP* (a gift from Karl Deisseroth).

The AAV-CBA-flAgRP-IRES-GFP and *AAV-CBA-GFP-WPRE* constructs were gifts from Roger Adan (University Medical Center Utrecht). *AAV-CAG-FLEx-EGFP* was a gift from Edward Boyden

(Massachusetts Institute of Technology Media Lab; Addgene plasmid #28304).

The Cre-dependent *AAV9-FLEx-GFP* was injected into the hippocampus of the *Pomc-Cre* mice to label the POMC-positive cells. *AAV5-DIO-hM3Dq-mCherry* was injected into the hippocampus of *Pomc-Cre* mice, allowing the receptor to be restrictively expressed and activated in the POMC neurons of the mouse hippocampus.

Supplemental References

Hitti, F.L., and Siegelbaum, S.A. (2014). The hippocampal CA2 region is essential for social memory. Nature *508*, 88-92.